Iranian Journal of Fisheries Sciences
http:doi.org/ 10.22092/ijfs.2025.133371 2025, 24(3) 473-504

Research Article

Production of a novel promising recombinant trypsin from *Fenneropenaeus merguiensis*: Towards biochemical and structural characterizations

Eskandari Mehrabadi M.[1], Hemmati R.[1, 2*], Homaei A.[3], Salemi Z.[4], Rigi G.[5]

1 Department of Biology, Faculty of Basic Sciences, Shahrekord University, Sharekord, Iran
2 Biotechnology Research Institute, Shahrekord University, Shahrekord, Iran
3 Department of Marine Biology, Faculty of Marine Science and Technology, University of Hormozgan, Bandar Abbas, Iran
4 Department of Biochemistry, Arak University of Medical Sciences, Arak, Iran
5 Department of Genetics, Faculty of Basic Sciences, Shahrekord University, Sharekord, Iran
*Correspondence: Roohullah.hemmati@sku.ac.ir; Hemmati1359@gmail.com

Keywords

Recombinant Trypsin,
Protease,
Banana shrimp,
E. coli Rosetta-gami

Article info

Received: May 2024
Accepted: October 2024
Published: May 2025

Abstract

This study presents the purification and characterization of novel recombinant trypsin derived from banana shrimp (*Fenneropenaeus merguiensis*) expressed in *E. coli Rosetta-gami*. The enzyme was purified using nickel sepharose chromatography and characterized through spectrophotometric kinetic and thermodynamic analyses, circular dichroism, and spectrofluorimetry. The cDNA encoding the putative trypsin, comprising 801 base pairs, was successfully isolated from the hepatopancreas of *F. merguiensis*. Sequence alignment of amino acids indicated a high degree of similarity (92-95%) with trypsins from *F. chinensis, P. vannamei, and F. mondon*. The purified recombinant trypsin exhibited a molecular weight of 23 kDa as determined by sodium dodecyl sulfate-polyacrylamide gel electrophoresis (SDS-PAGE). Optimal enzymatic activity was observed at pH 8 and 50 °C, with the enzyme demonstrating stability within a pH range of 7-9 and retaining approximately 50% of its initial activity across a temperature spectrum of 40-70 °C. The calculated half-life of the recombinant trypsin was 21.72 minutes at pH 8 and 50 °C. Kinetic parameters for casein as a substrate were determined, yielding K_m, V_{max}, k_{cat}, *and* k_{cat}/K_m values of 130.4 µg/ml, 0.0617 $\mu g \cdot min^{-1}.ml^{-1}$, 131.8 min^{-1}, and 1.01 $min^{-1}\mu g^{-1}$, respectively. Traditional methods for extracting trypsin from marine sources are inefficient. However, by utilizing recombinant DNA technology, we have produced a trypsin derived *F. merguiensis* with unique properties, including thermal stability and alkaline pH tolerance, highlighting its suitability for biotechnological applications.

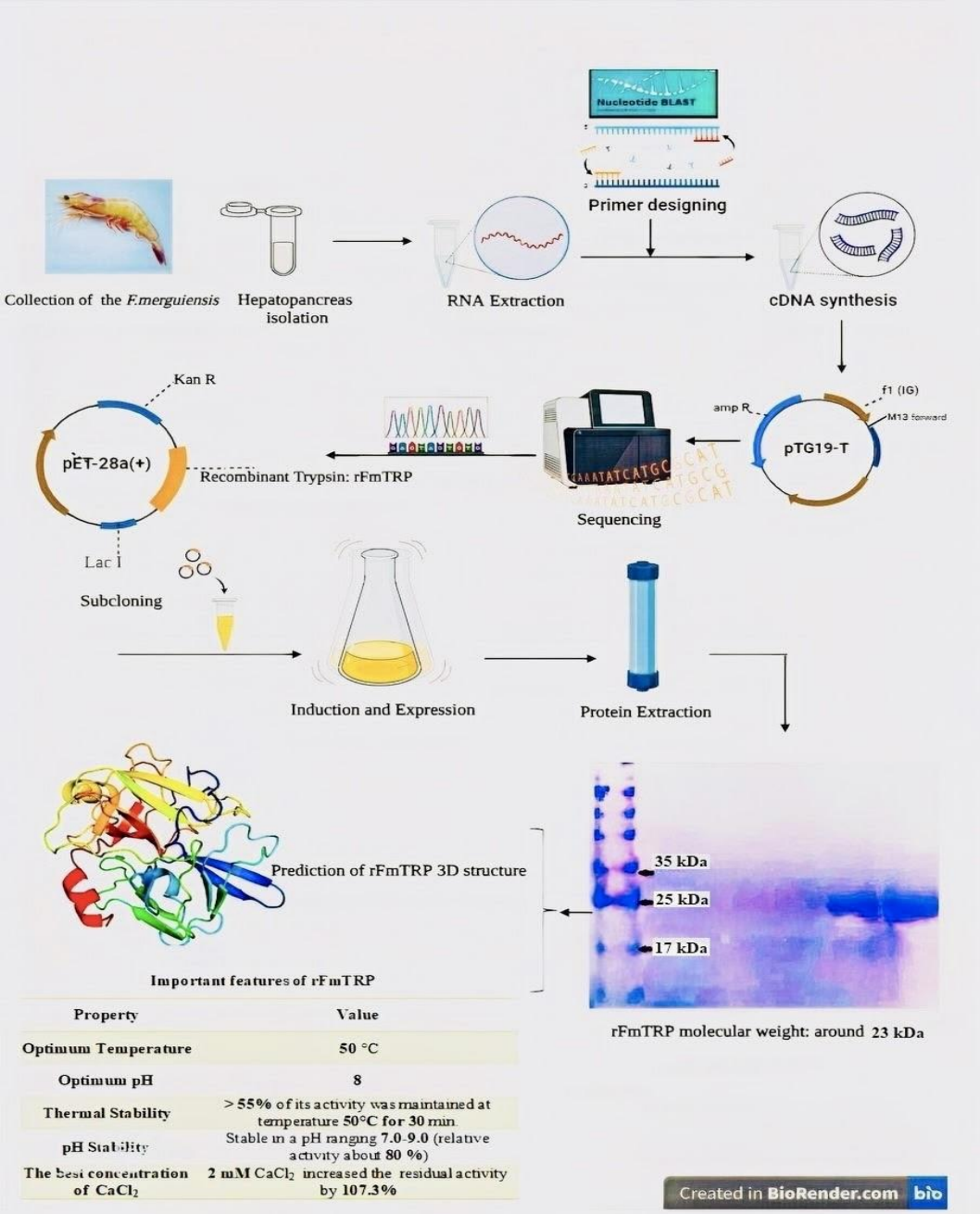

Graphical abstract

Introduction

Proteases are the largest group of industrial enzymes and have diverse applications in detergents, leather preparation, and food processing. During the last decade, marine proteases of non-microbial origin have been evaluated for applications in nutritional physiology and biochemistry (Klomklao *et al*., 2005). Aquatic animals have been adapted to different environmental conditions and these adaptations, along with interspecies and intraspecies genetic changes are related to the unique properties of their proteases compared to their counterparts from land animals, plants and microorganisms (Simpson, 2000; Klomklao, 2008). The hepatopancreas or midgut gland, located

within the digestive tract of marine crustaceans, is recognized for its elevated protolithic activity, which is responsible for the breakdown of food proteins. Among the various digestive enzymes of crustaceans, proteases have been studied the most (Gibson, 1979; Gimenez *et al*., 2001) Among the proteases, trypsin (E.C. 3.4.21.4) plays a key role in the digestion of dietary proteins in crustaceans, as it activates other zymogens and drives the digestion process (Tidwell and Allan, 2015; Eilertsen *et al*., 2018). The expression of trypsin in crustaceans is predominantly observed in various tissues, including hemocytes, stomach, hepatopancreas, and gills (Li *et al*., 2018). Production and activity of trypsin are regulated by several internal and external factors (Hernández and Murueta, 2009).

The study of trypsin properties is important due to the wide variation in kinetic and biochemical capabilities among different species, which may be correlated with their alimentary needs. The distinct features of trypsin derived from various crustacean species have been investigated and documented (Kim *et al*., 1994; Perera *et al*., 2020). Crustacean trypsin was also found to have unique structural features compared to other animal trypsin (Rawlings *et al*., 2018). The biochemical properties of crustacean trypsin are similar to those of trypsin from other animals, but they are more stable at higher temperatures (Perera *et al*., 2015). Bovine trypsin is a widely used enzyme in research laboratories and is the preferred choice for industrial protein processing and proteomic studies. Despite its popularity, shrimp trypsin has been found to possess a specific activity that is greater than bovine trypsin For example, Shrimp trypsin exhibits a particular activity that is 30 times greater than that of bovine trypsin I when measured at 25°C and a pH of 7.5 (Klein *et al*., 1996) and the midgut trypsins of *Penaeus monodon* exhibit a higher efficiency in the hydrolysis of various native proteins in vitro compared to bovine trypsin (Lu *et al*., 1990). As a result of their superior biochemical properties, marine-derived enzymes, such as shrimp trypsin, have emerged as promising alternatives to bovine trypsin, with significant implications for various biotechnological and industrial applications (Friedman and Fernández-Gimenez, 2023; Ghattavi and Homaei, 2023). Recombinant trypsin production has become an increasingly popular method due to the limitations of traditional trypsin extraction methods. Only few studies report the production of recombinant trypsin in various crustacean species. Guerrero-Olazarán *et al*. (2019) analyzed the purification and biochemical characterization of recombinant *P. vannamei* trypsinogen, with a particular focus on elucidating its activation kinetics (Guerrero-Olazarán *et al*., 2019).

The banana shrimp, *Fenneropenaeus mergueinsis (F. merguiensis)*, is classified taxonomically under the Penaeidae family, which is a family of marine crustaceans commonly known as penaeid shrimp. *F. merguie*nsis is widely distributed in the tropical and sub-tropical Indo-West Pacific (IWP) region (Vance and Rothlisberg, 2020). Due to its high demand as a food source, it is commercially important and extensively farmed in the fisheries and aquaculture industries (Dhani *et al*., 2020).

The biochemical characteristics of penaeid shrimp trypsin are not well known, because of the challenges associated with their isolation from natural sources (Sainz *et al*., 2004). Furthermore, it seems that prior to the data presented, expression of the active recombinant forms of other trypsin from shrimp has not been reported yet (Viader-Salvadó *et al*., 2013; Guerrero-Olazarán *et al*., 2019). In this study, we report the sequencing and molecular cloning of cDNA encoding trypsin *F .merguiensis* as well as the expression, purification, and characterization of the enzyme. In more detail, in the current study, in addition to the structural study of the novel trypsin from *F .merguiensis,* the biochemical properties of the enzyme including kinetics parameters, catalytic efficiency, pH stability, and thermal stability were characterized.

Materials and methods

Materials and Strains

Casein was purchased from Sigma-Aldrich, USA. All other chemicals were reagent grade and purchased from Merck, Germany. Taq DNA polymerase, Polymerase chain reactions (PCR) buffer, $MgCl_2$, dNTP, DNA ladder, M-MuLV reverse transcriptase, RNase inhibitor, oligoprimers, RNX-Plus solution for RNA extraction and T4 DNA ligase were purchased from Sinaclon, Iran. Bioneer's AccuPrep® gel purification kit was from Bioneer, Republic of Korea. XhoI and NcoI restriction enzymes were obtained from Thermo Fisher Scientific, USA and TA-cloning vector Kit was from Vivantis, Malaysia. SDS-PAGE analysis was performed using a Mini-PROTEAN electrophoretic system (BioRad) and the gels were stained with Comassie Brilliant Blue R-250 (Sigma-Aldrich, USA) (Wilson, 1983) to the molecular weight of the purified trypsin (Laemmli, 1970). *E. coli DH5α* , *BL21 (DE3),* and *Rosetta-gami* were prepared by the Iranian National Center for Genetic and Biologic Resources.

Culture media

For the cultivation of *E. coli* strains, Luria-Bertani (LB) medium composed of 5 $g.L^{-1}$ yeast extract, 10 $g.L^{-1}$ NaCl, and 10 $g.L^{-1}$ tryptone was used.

Sampling

White shrimps (*F. merguiensis*) were captured from the Persian Gulf, specifically the waters around Hormoz Island (27°05'N 56°27'E), using a trawl net in July 2018. Upon capture, shrimp hepatopancreas was promptly collected using a sterile scalping razor. The collected samples were then packed in aluminum foil and preserved by immersing them in liquid nitrogen. Subsequently, the preserved samples were stored in a freezer at –70°C until they were ready for analysis.

RNA extraction and cDNA synthesis

The total RNA was extracted using RNX-Plus solution (SinaClon Company, Iran). The RNA obtained was dissolved in 50 mL of diethyl pyrocarbonate water and stored at –80°C. The purity and integrity of the RNA were assessed by measuring the A260 and A260/280 ratios using an ultraviolet spectrophotometer (NanoDrop, EPOCH, Biotek, USA) and by performing agarose gel electrophoresis (1%). The RNA was then used as a template for cDNA synthesis. Specifically, 5 μg of DNase-treated RNA

was incubated with M-MuLV reverse transcriptase, RNase inhibitor, and the oligo(dT) primer (SinaClon Company, Iran) at a temperature of 42°C for one hour. Following the incubation, the reverse transcriptase was deactivated by heating the mixture to 80°C for 10 min. The quality of the resulting cDNA was assessed using 1% agarose gel electrophoresis. To analyze the RT-PCR-amplified cDNA of trypsin from *F. merguieinsis*, specific primers (Fig. 1) were used for agarose gel electrophoresis (1%).

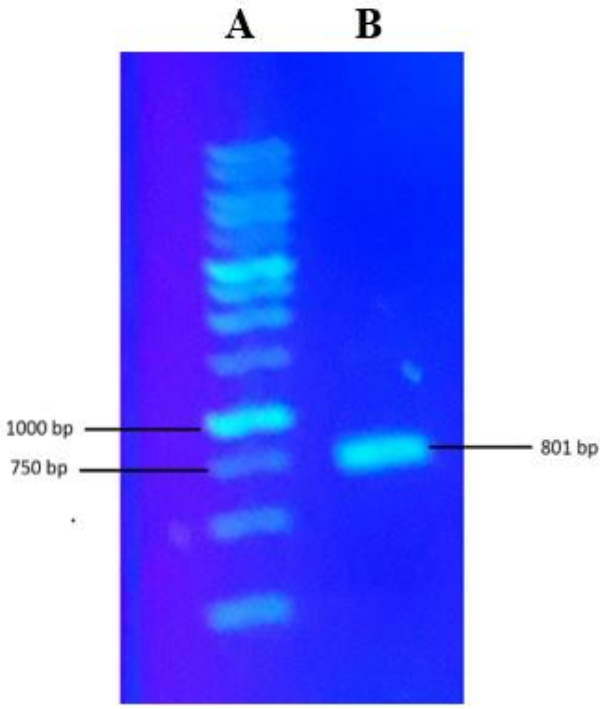

Figure 1: Agarose gel electrophoretic analysis (1%) of RT-PCR-amplified cDNA of trypsin from *F. merguieinsis* using specific primers (F1 and R1) from Table 1. Lane A: CinnaGen DNA Ladder 1 kb, Lane B: RT-PCR-amplified cDNA of trypsin from *F. merguieinsis.* Cycling was performed in a thermocycler (Applied Biosystems 2720) in calculated mode: 5 min initial denaturation at 95°C and 35 cycles of 40 s at 53°C, 2 min extension at 72 ◦C and 10 min final extension at 72◦C.

PCR conditions

PCR conditions were as follows: 5 min initial denaturation at 95°C and 35 cycles of 40 s at 53 °C, 2 min extension at 72°C and 10 min final extension at 72◦C in a thermocycler (Applied Biosystems 2720, Applied Biosystems, USA). The reaction mixture of a 20-µL final volume containing PCR buffer 10X, $MgCl_2$ 50 mM, dNTPs 10 mM, Taq DNA polymerase (5 unit/µL), and a pair of reverse and forward primers F1 (forward) and R1 (reverse) (Table 1) as well as 20ng trypsin encoding cDNA. PCR products were purified on agarose gel using Bioneer gel extraction kit (Bioneer, Republic of Korea).

TA cloning and sequencing

Trypsin encoding cDNA was amplified by PCR and then extracted and purified from agarose gel using Gel/PCR DNA extraction kit (Bioneer). The purified cDNA was ligated with pTG19-T vector using T4 DNA ligase. Next, the ligated mixture was prepared according to the manufacturer's instructions (Table 2). Subsequently, the

abovementioned PCR product was cloned into pTG19-T Vector (Kit TA cloning vector, Vivantis, Malaysia) (Fig. 2a).

Table 1: The sequence of primers used in the research.

Primer name	Sequence (5' - 3')	Target
F1	ATGAAGACCCTCATCCTCTGTGTGC	cDNA synthesis
R1	TTAAACAGCATTGGCCTTAATCC	
RXHO1	CCGCTCGAGAACAGCATTGGCCTTAATCC	Recombinant trypsin synthesis
FNCO1	CATGCCATGGCAATCGTCGGAGGAACTAACGCC	

Table 2: Condition of ligation reaction for TA-cloning.

pTG19-T vector (25ng/µL)	2 µL
The extracted PCR product	1 µL
10X Buffer Ligase	1 µL
T4 DNA Ligase (200u/µL)	1 µL
Nuclease-free	5 µL
Total Volume	10 µL

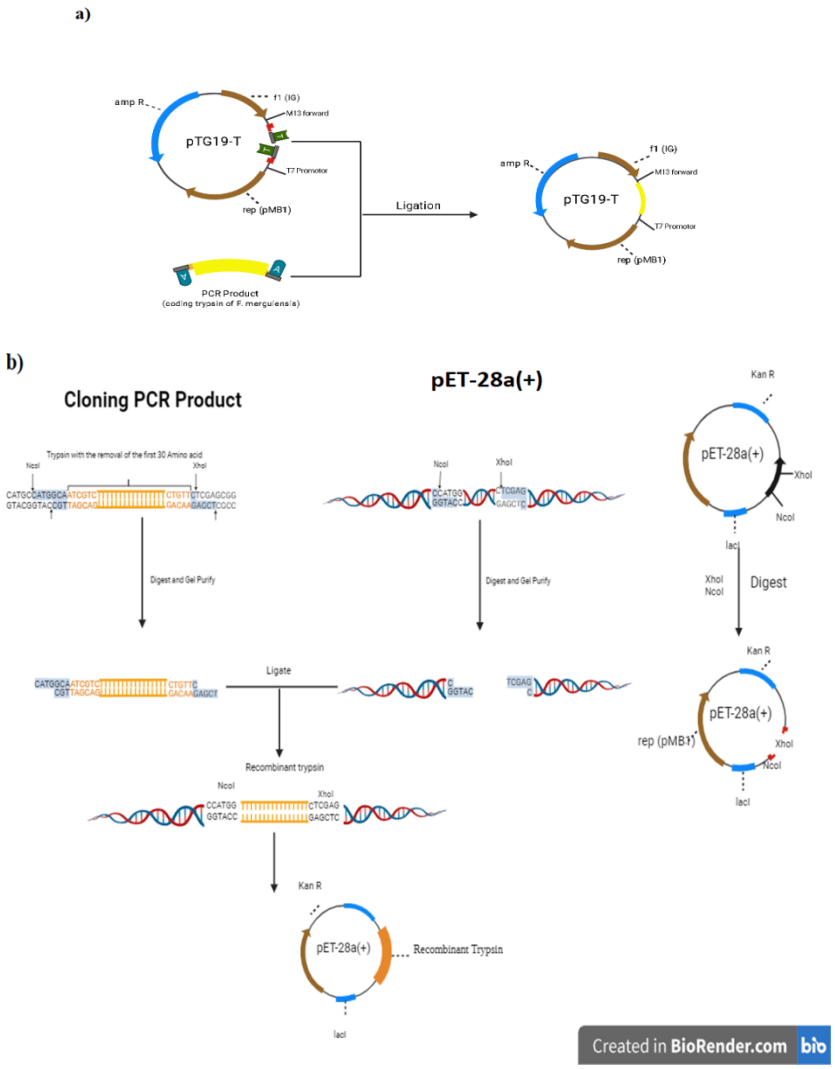

Figure 2: a) Schematic representation of the TA-Cloning process, b) Construction of an expression vector using XhoI and NcoI restriction enzymes.

Then, based on the manufacturer's instruction and transformed into *DH5α* competent cells. Transformants were screened by PCR and positive clones were sent to Faza Biotech Company for sequencing. After receiving sequencing results, the nucleotide sequence of the trypsin from *F. merguieinsis* was deposited in GenBank under accession no. MT232846. To check the codon compatibility index (CAI) and the commonness of codons we used accessible Rare Codon Analysis online tools (https://www.biologicscorp.com/tools/RareCodonAnalyzer/) (Fig. 3).

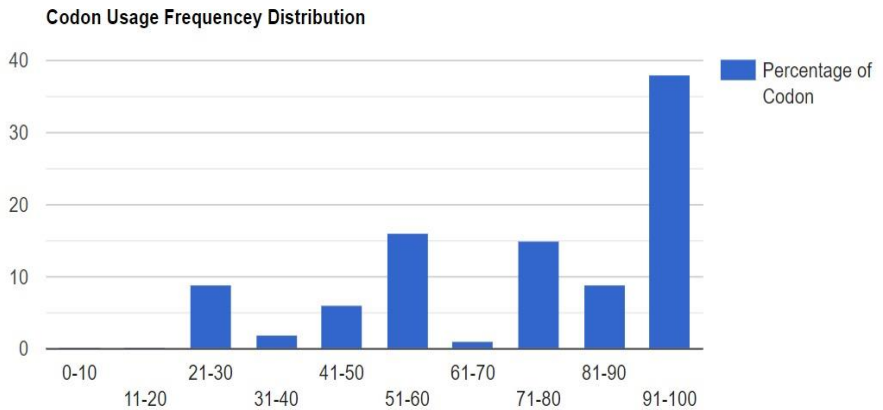

Figure 3: The result of Rare Codon Analysis to determine the codon compatibility index. (To predict the expression level of the desired protein in the selected host, you can use servers that check the codon adaptation index (Harp and Li, 1987) and Codon Frequency distribution. Rare Codon Analysis web software (https://www.biologicscorp.com/tools/RareCodonAnalyzer/) was used in this research.)

Construction of expression vector

Cloning primers containing *XhoI* and *NcoI* restriction site (RXHO1 and FNCO1, Table 1) were designed to delete the first 29 amino acids in N-terminal and add a methionine residue for translation initiation based on the pET28a (+) vector map. PCR conditions were as follows: 5 min initial denaturation at 95°C and 35 cycles of 45 s at 95°C, 60 s at 55°C, 2 min extension at 72°C and 10 min final extension at 72◦C in a thermocycler (Applied Biosystems 2720, Applied Biosystems, USA). The reaction mixture of a 10-µL final volume containing PCR buffer 10X, MgCl2 50 mM, dNTPs 10 mM, Taq DNA polymerase (5 unit/µL), and a pair of reverse and forward primers F1 (FNCO1) and R1 (RXHO1) (Table 1) as well as the purified pTG19-T vector after TA cloning. Purified PCR product of recombinant *F. merguiensis* trypsin *(*rFmTRP)and vector pET28a (+) were double digested by restriction enzyme *XhoI* and *NcoI* then were ligated to construct pET28a*rFmTRP* vector (For Construction of an expression vector, DNA fragment encoding trypsin and pET28a (+) vector digested with *XhoI* and *NcoI* restriction enzymes (Fig. 2b). The recombinant vector pET28arFmTRP transformed into *E. coli Rosetta-gami B(DE3)* by heat-shock treatment at 42°C and transformants of *E. coli Rosetta-gami_pET28arFmTRP* were obtained. The transformants were selected on LB plates

based on Kanamycin (KAN) resistance property (Li *et al*.). Then, the presence of DNA encoding trypsin in transformants was verified by colony PCR and the positive clones were identified and isolated. After the growth of positive bacterial clones, pET28a*Fm*TRP were extracted and digested with the restriction enzymes and analyzed on gel agarose electrophoresis to demonstrate the presence of inserted DNA fragment encoding trypsin and finally, the whole vector bearing novel trypsin was sequenced for more assurance.

Trypsin induction and purification

E. coli Rosetta-gami containing *pET28arFmTRP* were grown individually in 100 mL of LB medium with KAN 50 µg/mL and shaking 180 rpm overnight at 37°C. Then, 10 mL of the above culture was transferred to 180 mL of LB + KAN medium with shaking at 37°C until the OD600 reached 0.5 Protein expression was induced by adding 0.8 mM IPTG to the bacterial culture, which was grown further at 37°C for another 6 h. Then, cells were harvested by centrifugation at 6000×g for 20 min at 4°C and the resulting pellet was resuspended in 4 ml lysis Buffer (50 mM Tris-HCl, 150 mM NaCl, 20 mM imidazole, pH 7.5), disrupted by sonication, and centrifuged at 15000×*g* for 20 min at 4◦C. the supernatant was loaded onto Ni-Sepharose column (QIAGEN) with flow rate of 0.5 ml min^{-1}. Then, the column was washed with 20 mL of wash buffer (50 mM Tris-HCl, 150 mM NaCl, 60 mM imidazole, pH 7.4). Finally, proteins were eluted using an elution buffer containing (50 mM Tris-HCl, 150 mM NaCl, 220 mM imidazole, and pH 7.4). The collected fractions were analyzed by SDS-PAGE using standard protocols and fractions with the protein of interest were pooled. Protein concentration was determined using the Bradford colorimetric assay with bovine serum albumin (BSA) as the standard protein (Bradford, 1976).

Trypsin assay

Trypsin protease activity assayed at 50°C and the activity was measured in the presence of casein 1 g/dL as substrate according to the method presented in previous studies (Dadshahi *et al*., 2016). To assess the activity of rFmTRP, 0.468 ng of the purified enzyme was added to 1 mL of potassium phosphate buffer with a pH of 8 and incubated at 50°C in the presence of 10 g/dL casein and then the reaction was terminated by adding 1 mL of 10 g/dL TCA. The resulting mixture was centrifuged at 12000g for 12 min. Finally, the product absorption was read at 280 nm using a tyrosine standard curve by which the amount of product was calculated in terms of µg/min (UV/Visible Ultraspec Spectrophotometer, 1100 PRO Amersham Pharmacia Biotech Inc., UK).

Effects of pH and temperature on trypsin activity and stability

The effect of pH on enzyme activity was conducted in the same manner as the standard method, using sodium acetate (pH 3.0–5.0), sodium phosphate (pH 6.0–8.0), and glycine (pH 9.0–10.0) as reaction buffers (50 mM).

The pH stability of enzyme was measured after incubation of the rFmTRP

in the above-mentioned buffers (pH 3.0–10.0) at 37°C for 30 min. Samples were collected at 0, 15, and 30 min, and immediately placed on ice for 30 min. Then, trypsin activity was measured under pre-defined optimal conditions (50 mM potassium phosphate buffer, pH 8.0, and 50◦C).

To identify the optimal temperature, the activity of the purified enzyme was evaluated over a temperature range of 20°C to 90°C. The enzyme assay used a 50 mM potassium phosphate buffer with a pH of 8.0.

In order to analyze the thermal inactivation, the purified enzyme was incubated at various temperatures (20, 30, 40, and 50°C). Samples were collected from the enzymes that were incubated at different temperatures at 15-minute intervals and then placed on ice for 30 min. The residual activity was then measured at 50°C using a 50 mM potassium phosphate buffer with a pH of 8.0.

Thermodynamic parameters

Following the analysis of thermal inactivation, the thermal inactivation constant (kd) was determined by considering the slope of the plot depicting trypsin activity over time. Subsequently, the activation energy of the transition state $E^{\ddagger}_{a(D)}$was calculated by constructing an Arrhenius plot. Additionally, various thermodynamic parameters were calculated using the provided equations:

1. $\Delta G^{\ddagger}_{D} = -RT\ ln\ (kd \times h\ /kB \times T)$
2. $\Delta H^{\ddagger}_{D} = E^{\ddagger}_{a(D)} - RT$
3. $\Delta S^{\ddagger}_{D} = (\Delta H^{\ddagger}_{D} - \Delta G^{\ddagger}_{D})/\ T$
4. $t_{\frac{1}{2}} = ln\ 2/k_d$

Where, h = 6.63×10^{-34}J.s, $k_B = 1.38 \times 10^{-23}$J.K^{-1} and T is temperature (Kelvin), R = 8.314 JK^{-1}mol^{-1}.

Kinetic parameters

To determine the kinetic parameters (including the maximum velocity *(V_{max}) and* Michaelis-Menten constant *(K_m)*, Values of turnover number (k_{cat}) of the purified rFmTRP, steady-state kinetic studies were conducted. 0.468 ng of the purified enzyme was added to 1 mL of potassium phosphate buffer (pH = 8) and enzyme activity was assayed in the presence of different concentrations (1 g/dL) of casein-substrate under assay conditions at 50°C. The values of K_m, k_{cat} and k_{cat}/K_m were determined by non-linear regression approximation from Michaelis–Menten plots using Prism software (version 9). The value of turnover number (k_{cat}) was calculated from the following equation: $V_{max}/[E_t] = k_{cat}$, where [E_t] refers to the total active enzyme concentration in the reaction. Each sample was repeated 3 times.

Far UV circular dichroism (CD) spectroscopy analysis

For structural studies using CD, it is crucial to eliminate imidazole from the enzyme environment to minimize noise interference. To achieve this, dialysis was carried out using a phosphate buffer (50 mM KPO4, pH 7.8) as the dialysis buffer, supplemented with ١%glycerol, 150 mM NaCl, 1 mM DTT, 1 mM EDTA, 0.8 mM ammonium sulfate, and 2 mM beta mercaptoethanol. The dialysis was performed at 4°C with magnetic steering

for 10 hours in a 1-liter buffer volume. The dialysis buffer was replaced every two hours during the dialysis process. Subsequently, the trypsin concentration of the samples was determined using the Bradford test. The secondary structure of protein rFmTRP was analyzed using Far-UV CD measurement. The protein samples were placed in a 1 mM wide sample cell and scanned using a Jasco J-810 Circular Dichroism Spectropolarimeter at a rate of 20 nm.min−1. The measurement was conducted in the far-UV region, specifically within the wavelength range of 190–240 nm, at room temperature. To ensure accuracy, the CD instrument was calibrated using a d-10 camphor sulfonic acid aqueous solution. The obtained CD spectra were corrected for background by subtracting the spectra of reference samples, which included the inducers and buffer. The CD spectra were recorded at 25 °C using a 2-mm path length cuvette and represent the average of 3 scans by smoothing data in graphpad prism.

Intrinsic fluorescence of rFmTRP

Using a fluorescence spectrophotometer, the intrinsic fluorescence measurements were carried out. The emission spectra were recorded in the range of 300-450 nm, whereas the excitation wavelength of the fluorescence spectrum was set at 290 nm. Excitation and emission slit bond widths have been adjusted at 10 nm and 3 nm, respectively. Every study was conducted using quartz cells that contained 0.2 mg/mL rFmTRP. Using phosphate buffer (50 mM KPO4, pH 7.8) as the dialysis buffer and adding 1% glycerol, 150 mM NaCl, 1 mM DTT, 1 mM EDTA, 0.8 mM ammonium sulfate, and 2 mM beta mercaptoethanol, the fluorescence emission spectra of trypsin were examined.

Bioinformatics analysis and homology modeling of rFmTRP

The complete nucleotide sequence of *F. merguiensis* trypsin was obtained and submitted to the National Center for Biotechnology Information (NCBI) (https://www.ncbi.nlm.nih.gov/) and registered under the accession number MT232846.1. The results showed that the full-length cDNA of trypsin from *F. merguiensis* contain 801 bp. Translated rFmTRP cDNA sequence (*F. merguiensis* trypsin after removal of 29 amino acids from signal peptide) has 238 amino acid residues. The amino acid sequence of rFmTRP was subjected to a similarity search in UniProt (https://www.uniprot.org/blast/) and NCBI (Altschul *et al*., 1997) databases by BLASTp tool to find similar sequences. Multiple alignments of the amino acid sequences of *rFmTRP* and its homologous proteins was done using the Clustal Omega program (https://www.ebi.ac.uk/Tools/msa/clustalo/) (Sievers and Higgins, 2018; Madeira *et al*., 2019) and eventually, the results were analyzed by Jalview 2.8. The evolutionary relationship and phylogenetic analysis were inferred using the Neighbor-joining method (Saitou and Nei, 1987), and a phylogenetic tree was conducted using MEGA 11 software (Kumar *et al*., 2004). All sequences used in the phylogenetic analysis are listed in Table 3**.** A fully automatic procedure with I-TASSER server was used to construct a 3D structural model of the deduced protein by homology modeling (Yang and Zhang, 2015) using the available crystal structures.

Table 3: Sequences producing significant alignments.

Description	Scientific Name	Amino acid Length	Accession
trypsin-1-like [*Penaeus chinensis*]	*Penaeus chinensis*	266	XP_047473697.1
trypsin [*Penaeus merguiensis*]	*Penaeus merguiensis*	266	QKO29468.1
trypsin-1-like [*Penaeus monodon*]	*Penaeus monodon*	266	XP_037776552.1
trypsin, partial [*Penaeus vannamei*]	*Penaeus vannamei*	263	CAA75311.1
trypsinogen 1 [*Penaeus vannamei*]	*Penaeus vannamei*	266	AEZ67461.1
trypsin-1-like [*Penaeus vannamei*]	*Penaeus vannamei*	266	XP_027232277.1
trypsin, partial [*Penaeus chinensis*]	*Penaeus chinensis*	183	AAT09988.1
trypsin, partial [*Euphausia pacifica*]	*Euphausia pacifica*	185	ABQ02518.1
trypsin, partial [*Penaeus chinensis*]	*Penaeus chinensis*	185	ABQ02525.1
trypsin, partial [Euphausia superba]	*Euphausia superba*	185	ABQ02523.1
trypsin, partial [*Euphausia pacifica*]	*Euphausia superba*	185	ABQ02517.1
trypsin, partial [*Penaeus chinensis*]	*Penaeus chinensis*	185	ABQ02530.1
trypsin, partial [*Penaeus chinensis*]	*Penaeus chinensis*	185	ABQ02528.1
Trypsin, partial [*Pacifastacus leniusculus*]	*Pacifastacus leniusculus*	268	CAA10915.1
hepatopancreas trypsin, partial [*Astacus leptodactylus*]	*Astacus leptodactylus*	237	AAX98287.1
trypsin-1-like isoform X2 [*Eriocheir sinensis*]	*Eriocheir sinensis*	267	XP_050731400.1
trypsin-1-like [*Portunus trituberculatus*]	*Portunus trituberculatus*	261	XP_045134072.1
trypsin-1-like isoform X3 [*Eriocheir sinensis*]	*Eriocheir sinensis*	261	XP_050731401.1
trypsin-1-like [*Eriocheir sinensis*]	*Eriocheir sinensis*	261	XP_050731407.1
trypsin 1b [*Panulirus argus*]	*Panulirus argus*	266	ADB66712.1
trypsin [*Penaeus vannamei*]	*Penaeus vannamei*	249	ROT79324.1
trypsinogen 2 [Penaeus vannamei	*Penaeus vannamei*	270	ROT68888.1
trypsinogen 2 [*Penaeus vannamei*]	*Penaeus vannamei*	270	ROT68896.1
trypsin-1-like isoform X2 [*Penaeus chinensis*]	*Penaeus chinensis*	266	XP_047472830.1

Results

Molecular identification and sequencing of rFmTRP

The cDNA sequence encoding *F. merguiensis* trypsin was synthesized using trypsin mRNA obtained from the hepatopancreas tissue of *F. merguiensis*. The synthesized cDNA sequence was then cloned into recombinant vectors pTG19-t and sequenced. The complete nucleotide

sequence of rFmTRP was obtained and submitted to NCBI GenBank under the following accession number MT232846.1. The mRNA from *F. merguiensis* subcloned into pET28a (+) to obtain pET28aFmtrp *E. coli Rosseta-gami* competent cells were transformed with pET28arFmTRP.

Bioinformatics analysis

By protein sequence blast of rFmTRP, similar sequences of trypsin-I-like protein were found. The multiple sequence alignment of rFmTRP and other similar proteins was performed by a Clustal Omega program (Fig. 4). The analysis of rFmTRP amino acid residues with similar shrimp trypsin protein sequences using BLAST software showed the highest similarity with *F. chinensis*, *P. vannamei*, and *F. mondon* species with a percentage of similarity (respectively) 95.76, 94.63 and 92.51%.

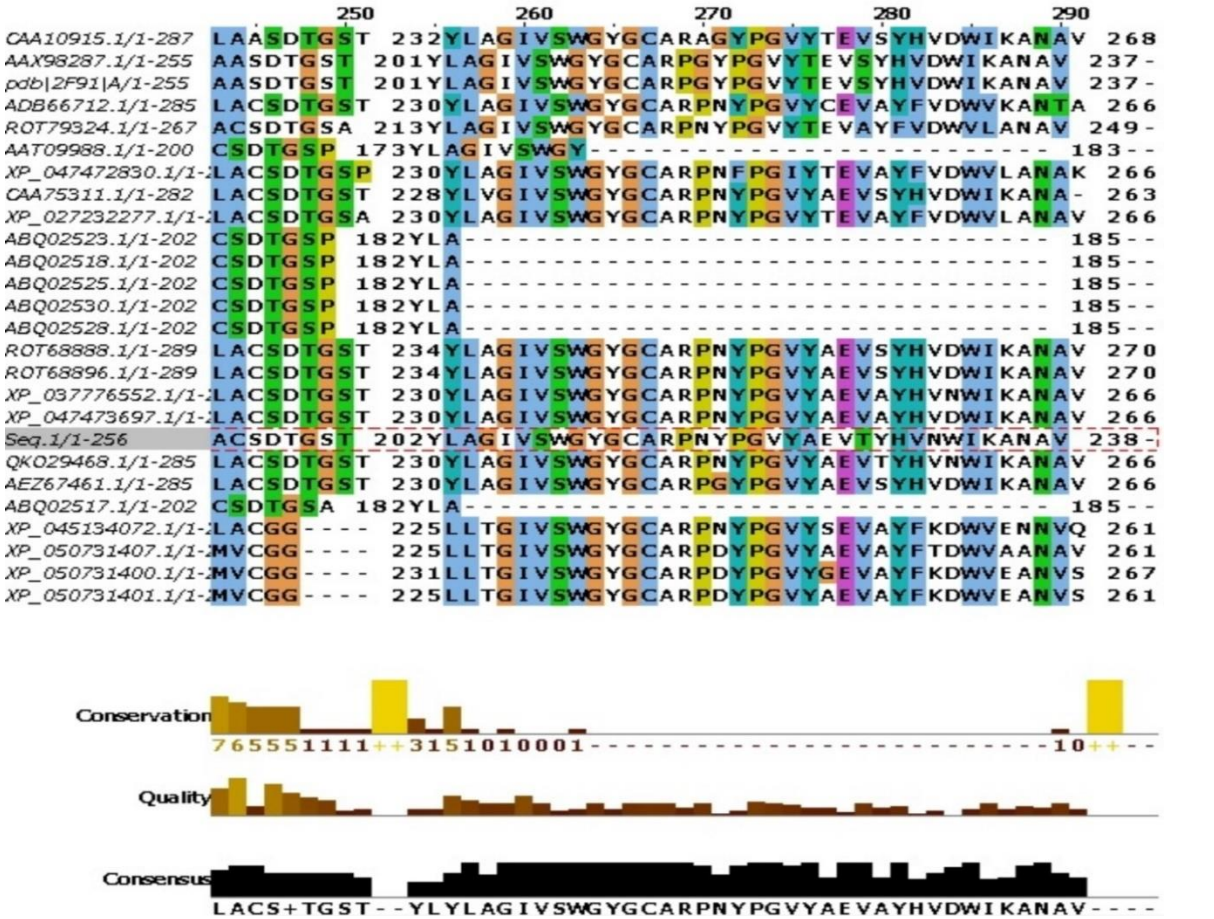

Figure 4: Multiple sequence alignment of rFmTRP and its homologous. The multiple sequence alignment was performed by Clustal Omega program. The sequences are labeled with original given names, followed by the UniProt ID.

Phylogenetic and evolutionary analysis of trypsin and its homologues

Using the Neighbor-joining tree method of Mega 11 software, the evolutionary relationships and phylogenetic tree of rFmTRP and other 25 homologous were constructed (Fig. 5).

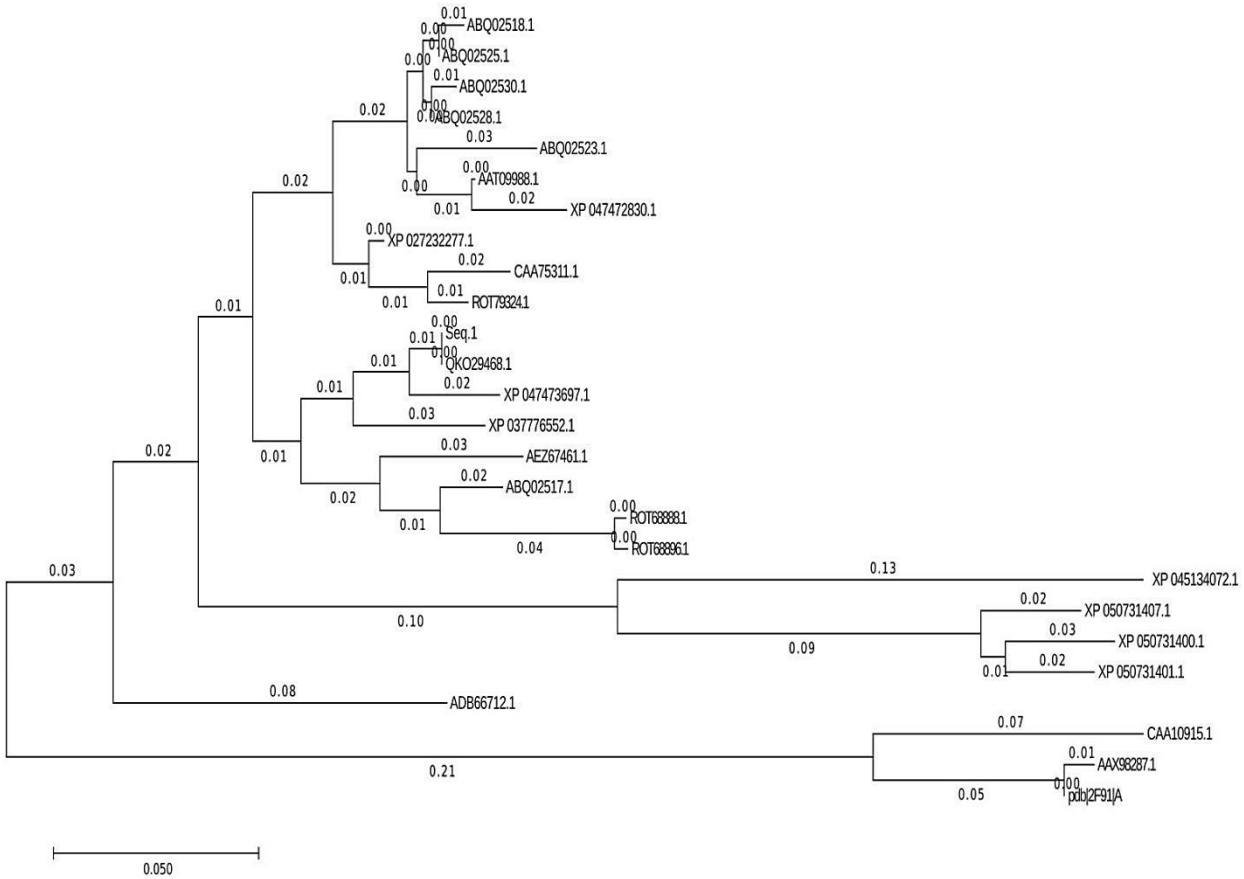

Figure 5: The evolutionary relationships of rFmTRP with its homologous proteins. The evolutionary history of trypsin and its homologous protein was inferred using the Neighbor-Joining method. Evolutionary analyses were conducted in MEGA 11.

The numbers next to each node represent bootstrap values for 1000 replicates. Neighbor-joining tree indicates that these rFmTRP are divided into two main groups. There are 23 members in the first group, including a trypsin species from *F. merguiensis*. The second group includes 3 members including *F. merguiensis trypsin*. This evolutionary relationship indicates that *F. merguiensis* trypsin is clustered with the >QKO29468.1. The results of phylogenetic tree analysis showed that *F. merguiensis* trypsin had the lowest gene distance (0.03) from trypsin-I-like *Penaeus chinensis* (XP_ 047473697.1) and (0.049) trypsin-/-like *Penaeus monodon* (XP 037776552.1). This result also showed that it has a higher correlation with trypsin-like serine proteinase 2 and trypsin 1-like *P. chinensis* species with a strong bootstrap of 82%.

Trypsin from *F. merguiensis* contains a 15-amino acid signal peptide at the N-terminal end (MKTLILCVLVAGAFA) indicating that it is a secretory enzyme. The peptide contains a high proportion of hydrophobic residues along with an alanine as the terminal amino acid, which is the typical characteristic of eukaryotic signal sequence. Remaining subsequent 14 N-terminal amino acids comprise a trypsin activation domain, which must be removed to have an active enzyme with IVGG at N-terminal sequence. The activation domain

is found in various arthropoda and crustacean species (Klein *et al*., 1998; Hernández-Cortés *et al*., 1999; Kvamme *et al*., 2004; Rudenskaya *et al*., 2004). We have removed the sequence encoding signal peptide in the recombinant construct to bypass the subsequent proteolytic cleavage of the signal peptide as a key step for enzyme activation. In other words, the aim of the removal of the signal peptide is to quickly access the active enzyme as well as reduce costs and save time. According to the analysis of sequence alignment, full sequences of *F. merguiensis* trypsin had a considerable similarity with the heat-tolerant counterparts and exhibited many highly conserved sites. One of the important sites in the active site includes H-D-S (histidine, aspartic acid and serine). In more detail, three residues based on the conserved domain of Tryp_SPc (the conserved domain of Tryp_SPc refers to a specific sequence of amino acids that is found in the trypsin superfamily of serine proteases) (Li *et al*., 2012) His 46, Asp97 and Ser 190 are key residues involved in catalysis.

The primary specificity of trypsin is to cleave peptide bonds on the carboxyl side of basic amino acids including lysine or arginine (Stryer, 1988). The primary specificity of trypsin is determined by three residues, two of which are Gly (216 and 226 chymotrypsin numbering) on the binding pocket's wall, allowing access to bulky residues such as Arg and Lys, while Asp189 (chymotrypsin numbering) stabilizes their basic side chains near the pocket's bottom (Perona and Craik, 1995). The conservation of 3 residues involved in the proteolytic cleavage is evident in Figure 6, where all the sequences of trypsin from different species of shrimp contain an Asp212 residue near the substrate-binding pocket's base to stabilize the positive charge of P1 Arg or Lys side chains. Additionally, Gly239 and Gly249 are located on one side of the pocket in all shrimp species. Try192 and Ser213 residues can determine secondary specificity. Try192 is conserved in all trypsins from *P. argus, L. vannamei, and Lepeophtheirus salmonis* (Perera *et al*., 2010). Furthermore, Ser190 (Ser213 in all trypsins from shrimps and the most of trypsins from lobsters) in bovine trypsin forms a hydrogen bond with P1-Arg side chain, and its replacement can affect the preference for Arg versus Lys (Evnin *et al*., 1990). The calcium-binding motif has been found in decapods crustaceans. It is unclear whether calcium ions are necessary for invertebrate trypsins to work optimally or to remain stable (Muhlia-Almazán *et al*., 2008a). The presence of this calcium-binding motif was determined in the full-length sequence of trypsin from *F. merguiensis*. As depicted in Figure 6, calcium-binding motif can be observed. In line with this finding, the effects of calcium concentration on enzyme activity were investigated and reported in the 3.9 subsections. According to our results, NetNGlyc (http://www.cbs.dtu.dk/services/NetNGlyc/) and GlycoEP (https://webs.iiitd.edu.in/raghava/glycoep) servers found one potential N-glycosylation site Asn55 (which is equivalent to Asn83 in the full-length sequence of trypsin from *F. merguiensis*) and the presence of Pro residue just after Asn residue (NPDY) makes the possibility of N-glycosylation

highly unlikely due to structural constraints and thus, the possibility of N-glycosylation of rFmTRP seems weak. However, the possibility of O-glycosylation sites can be predicted in full-length sequence of trypsinogen (Ser18 and Thr22).

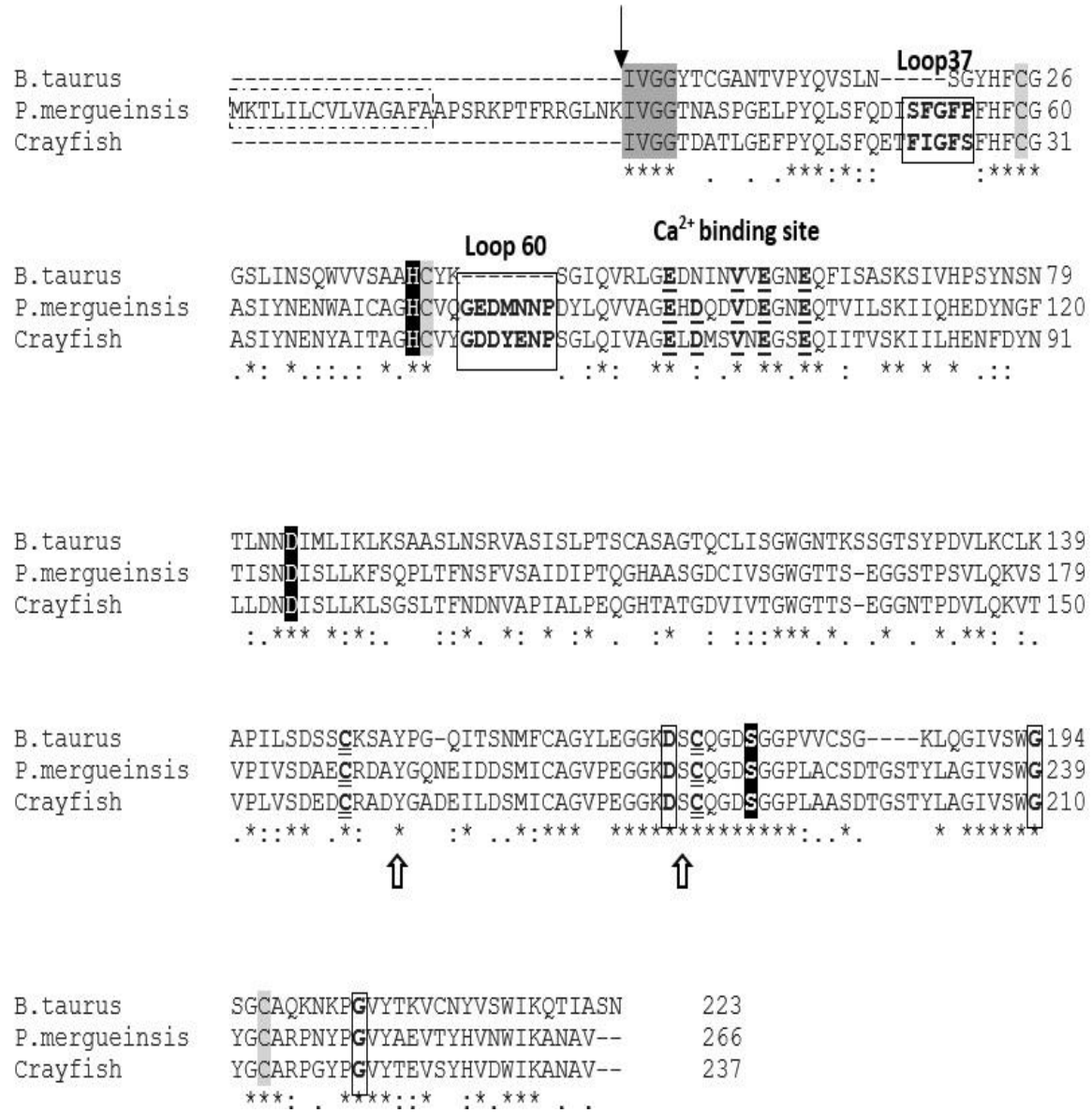

Figure 6: Alignment of fully sequences of *F. merguiensis* trypsin with *crayfish* (PDB code: 2f91A) and *bovine* (PBD code: 2ftlE). The aligned sequences highlight conserved residues, signal peptides, and the activation peptide cleavage site. Additionally, the N-terminal residues of mature enzymes and cysteine residues in predicted disulfide bridges are shaded in dark and light grey, respectively. The catalytic triad (His74, Asp125, and Ser218) is represented by black shaded white letters. Primary specificity determinants are boxed with a continuous line, while secondary determinants are indicated with white-headed arrows at the bottom of sequences. Notably, residues forming the calcium-binding site are in bold, and differences in two of the superficial loops are boxed and indicated according to Fodor et al.'s (Fodor *et al.*, 2005) nomenclature. The numbering of residues starts at the first residue of proteins (Perera *et al.*, 2010).

To investigate the three-dimensional structure of enzyme, I-TASSER server (Yang and Zhang, 2015) was employed to generate five models, with the best model

given the values of -0.25 and 0.87+-0.07 for overall C-score and TM-Score, respectively and RMSD estimated to be 3.5+-2.4. The value of C-score is a confidence score for estimating the quality of predicted models by I-TASSER. It is calculated based on the significance of threading template alignments and the convergence parameters of the structure assembly simulations. The value of C-score is typically lies in the range of [-5, 2], where a C-score of higher value signifies a model with high confidence and vice-versa. A 3D structural model of of rFmTRP by using I-TASSER server was depicted in Figure 7.

Figure 7: 3D structural model of of rFmTRP by using I-TASSER server according to homology modeling based on the available crystal structures.

Moreover, Hydrophobicity/ Hydrophilicity of the amino acids consisting the novel trypsin was determined using the peptide2 server (https://www.peptide2.com/N_peptide_hydrophobicity_hydrophilicity.php) and the results are as follows: Hydrophobic: 37.82%, Acidic: 12.18%, Basic: 5.46%, Neutral: 44.54%.

Next, the solubility of the novel trypsin was predicted by protein-sol server (https://protein-sol.manchester.ac.uk/) according to a sequence-based program and the value of the predicted scaled solubility was estimated to be 0.628. According to the experimental solubility dataset, the values of scaled solubility greater than 0.45 have a higher solubility compared to the soluble proteins of *E. coli* (Hebditch *et al*., 2017). The physicochemical characteristics of rFmTRP were assessed utilizing the ProtParam. The ProtParam tool requires a peptide sequence containing a minimum of 5 amino acid residues as input and calculates various parameters such as the number of amino acids, molecular weight, theoretical isoelectric point (pI), extinction coefficient, amino acid composition, half-life, aliphatic index, instability index, grand average of hydropathicity (GRAVY) score, number of positively charged residues, number of negatively charged residues, and atomic composition. The analysis was performed using the web-based version of the ProtParam tool available at (https://web.expasy.org/protparam/) (Fig. 8).

According to the calculated results, the predicted molecular weight of rFmTRP is 25 KDa and the calculated theoretical isoelectric point (Bjellqvist *et al*., 1993) of rFmTRP is calculated to be 4.13. The protein sequence of rFmTRP is composed of the highest percentage of amino acids (11.8%) of Gly and Ser (9.7%), Val (7.6%), Val (7.5%), and Ile, Ala and Asp (7.1%). In addition, the aliphatic index is estimated to be 73.32.

Expression and purification of trypsin from rFmTRP

The recombinant N-terminal His6-tagged expressed in *E. coli Rosetta-gami* cells was purified. Our purified rFmTRP fraction showed a molecular mass in SDS-PAGE around 23 kDa (Fig. 9), which is approximately in agreement with the theoretical MW calculated based on the primary amino acid sequence (25 kDa).

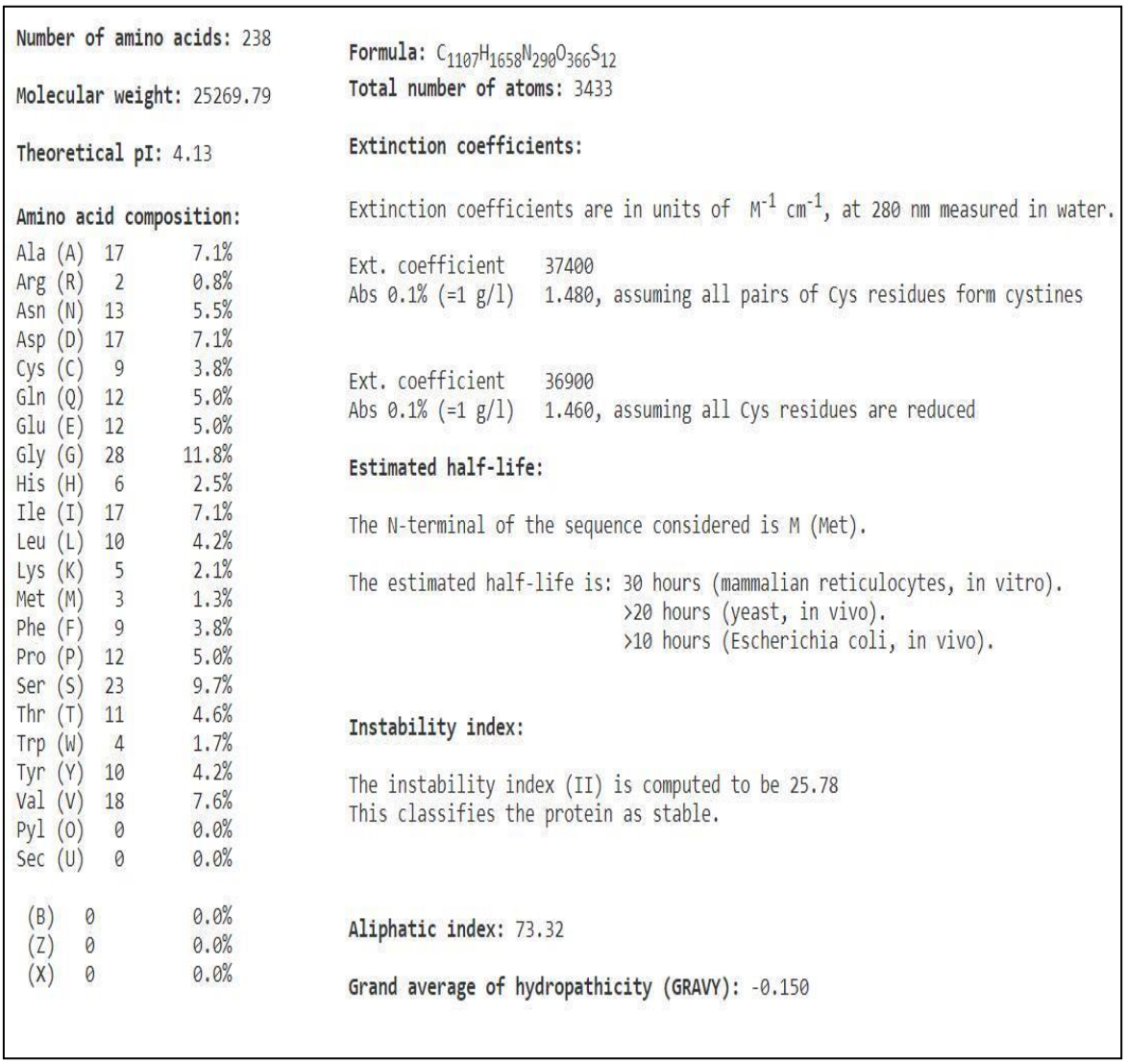

Number of amino acids: 238

Molecular weight: 25269.79

Theoretical pI: 4.13

Amino acid composition:

Ala (A)	17	7.1%
Arg (R)	2	0.8%
Asn (N)	13	5.5%
Asp (D)	17	7.1%
Cys (C)	9	3.8%
Gln (Q)	12	5.0%
Glu (E)	12	5.0%
Gly (G)	28	11.8%
His (H)	6	2.5%
Ile (I)	17	7.1%
Leu (L)	10	4.2%
Lys (K)	5	2.1%
Met (M)	3	1.3%
Phe (F)	9	3.8%
Pro (P)	12	5.0%
Ser (S)	23	9.7%
Thr (T)	11	4.6%
Trp (W)	4	1.7%
Tyr (Y)	10	4.2%
Val (V)	18	7.6%
Pyl (O)	0	0.0%
Sec (U)	0	0.0%
(B)	0	0.0%
(Z)	0	0.0%
(X)	0	0.0%

Formula: $C_{1107}H_{1658}N_{290}O_{366}S_{12}$

Total number of atoms: 3433

Extinction coefficients:

Extinction coefficients are in units of M^{-1} cm^{-1}, at 280 nm measured in water.

Ext. coefficient 37400
Abs 0.1% (=1 g/l) 1.480, assuming all pairs of Cys residues form cystines

Ext. coefficient 36900
Abs 0.1% (=1 g/l) 1.460, assuming all Cys residues are reduced

Estimated half-life:

The N-terminal of the sequence considered is M (Met).

The estimated half-life is: 30 hours (mammalian reticulocytes, in vitro).
>20 hours (yeast, in vivo).
>10 hours (Escherichia coli, in vivo).

Instability index:

The instability index (II) is computed to be 25.78
This classifies the protein as stable.

Aliphatic index: 73.32

Grand average of hydropathicity (GRAVY): -0.150

Figure 8: Prediction of the physicochemical properties of rFmTRP by ProtParam tool (https://web.expasy.org/protparam/)

CD spectrum of rFmTRP

The content of the secondary structure of the rFmTRP was estimated from the CD spectrum (Fig. 10). The best estimation calculated based on the data obtained from the website http://dichroweb.cryst.bbk.ac.uk/ and summarized in Table 4. For the prediction of the second structure of rFmTRP, the protein secondary structure prediction server jpred[4] (https://www.compbio.dundee.ac.uk/jpred4/index.html) was used (Fig. 11).

Intrinsic fluorescence analysis of rFmTRP

The fluorescence emission spectrum in the range of 300-450 nanometers has been investigated. When the protein is excited at a wavelength of approximately 290 nanometers, the intrinsic fluorescence originates from the remaining tryptophan and tyrosine residues, and this intrinsic fluorescence is highly sensitive to the environment (Sun *et al*., 2002). Therefore, changes in intrinsic fluorescence can reflect whether the protein structure has changed (Zhou *et al*., 2009). The intensity of fluorescence depends on whether tryptophan is located in a hydrophobic environment within the protein structure during protein folding or exposed at the surface upon protein unfolding. The intrinsic fluorescence intensity of *rFmTRP* is highest at a wavelength of 344.5 nanometers. Under these conditions, it appears that the tryptophan in residues *rFmTRP* is significantly buried inside the protein and have less contact with the aqueous environment (Fig. 12).

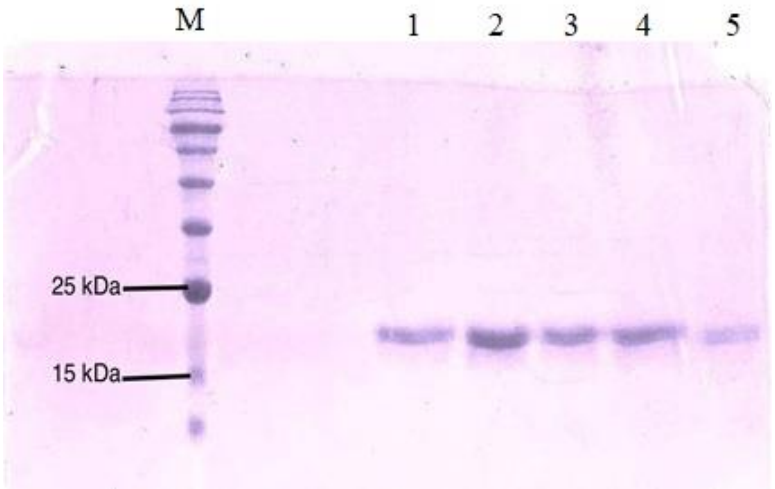

Figure 9: SDS-PAGE analysis of rFmTRP obtained by the different purification steps (~23 kDa). Proteins were detected by Coomassie brilliant blue on SDS-PAGE 12.5%. Lane 1: Eluted Fraction 1; Lane 2: Eluted Fraction 2; Lane 3: Eluted Fraction 3; Lane 4: Eluted Fraction 4; Lane 5: Eluted Fraction 5 and Lane M is the molecular mass marker.

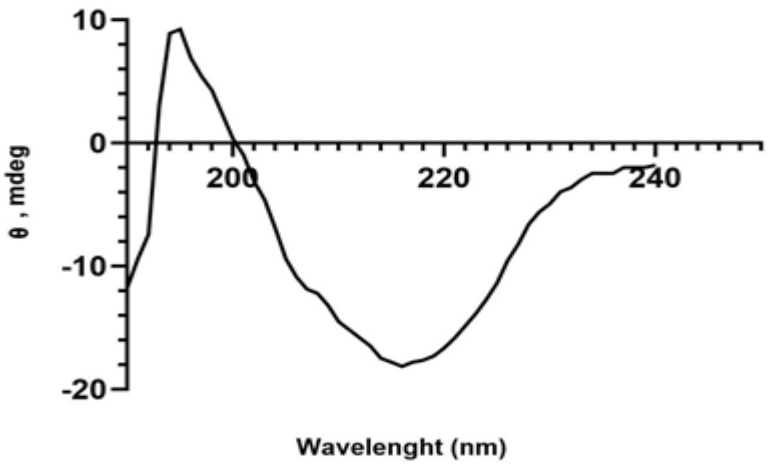

Figure 10: Far-UV CD spectra. Plots of ellipticity between 190 and 240 nm for rFmTRP. Protein concentration in phosphate buffer (50 mM KPO4, pH 7.8) was 200µg/ml (After dialysis). The spectra were recorded at 25°C in a cuvette of 2-mm path length and represent the average of 3 scans by smoothing data in graphpad prism version 9. The best estimate obtained based on the information and calculations obtained from the site (http://dichroweb.cryst.bbk.ac.uk).

Table 4: The best estimate of second structures obtained based on the information and calculations from the site http://dichroweb.cryst.bbk.ac.uk.

Results	α-helix	distorted α-helix	regular β-strand	distorted β-strand	Turns	Unordered	Total
Final	0.034	0.067	0.220	0.142	0.152	0.382	1.0

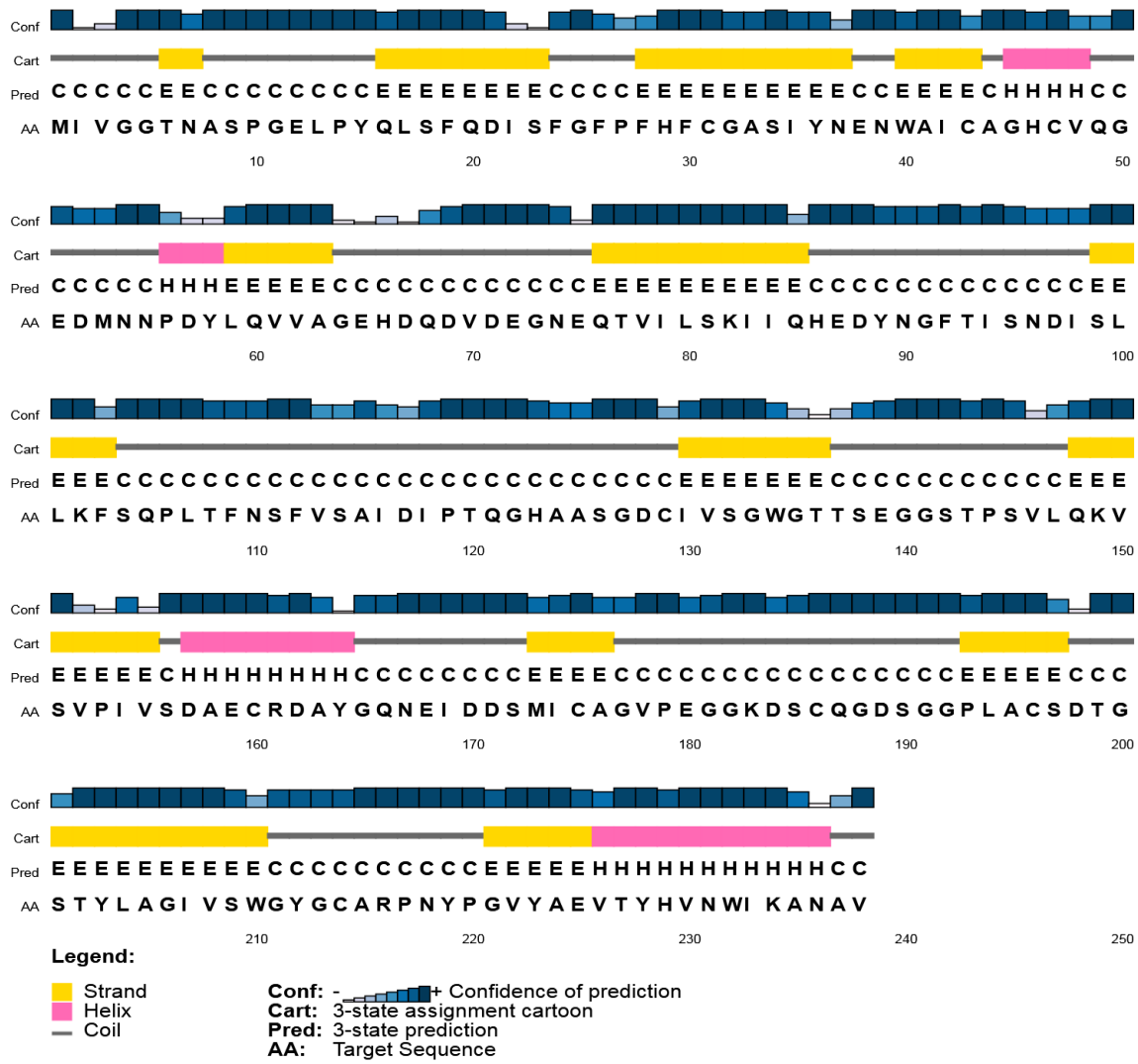

Figure 11: Prediction of the second structure of rFmTRP using the protein secondary structure prediction server jpred[4] (https://www.compbio.dundee.ac.uk/jpred4/index.html).

Effect of pH and temperature on enzyme activity and stability

The pH profile of *rFmTRP* is shown in Figure 13a, the optimum pH of rFmTRP for casein hydrolysis is 8. The pH stability of *rFmTRP* is shown in Figure 13b. Based on the results, rFmTRP is stable in a pH value ranging from 7.0 and 9.0 (relative activity about 80%) and a decrease in the activity at pH values less than 6 is considerable. However, a slight decrease in activity is observed at pH higher than 9. It is worthy to note that a remarkable decrease in the activity can be seen at pH value of 3 (relative activity about 10%). Inversely, trypsin shows higher activity at higher basic

pH values ranging from 5.0 and 11.0 (relative activity about 40 %). From Figure 13c, where the effect of temperature on the activity of rFmTRP is shown (each value is the mean of three independent experiments), it appears that the optimum temperature of rFmTRP for hydrolysis of casein is 50°C. However, due to the thermal deactivation of trypsin, the activity decreases at temperatures above 65°C. As depicted in Figure 13d, according to the results of thermal inactivation of purified rFmTRP, the activity of rFmTRP at 50°C after 15 and 30 min respectively, shows 66% and 55% stability.

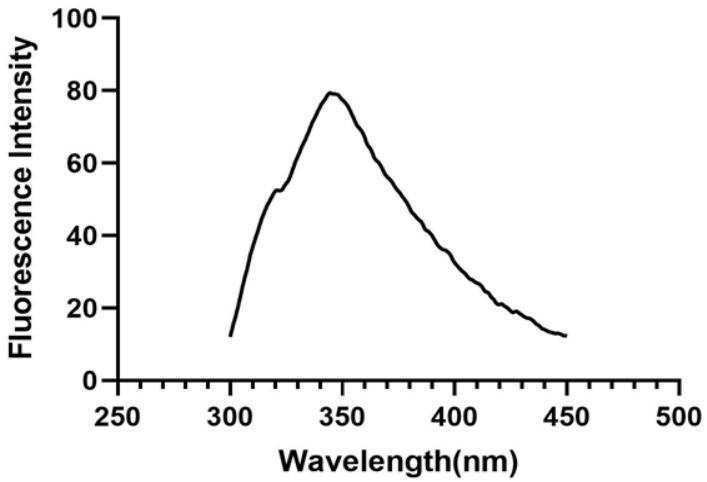

Figure 12: Intrinsic fluorescence spectrum of *rFmTRP*. Fluorescence emission spectrum at 300-450 nm has been investigated. When the protein is excited at a wavelength of about 290 nm, the intrinsic fluorescence of the *rFmTRP* is the highest at a wavelength of 344.5 nm. In this situation, it seems that the tryptophan roots are significantly placed inside the protein and have less contact with the aqueous environment.

Kinetic parameters of rFmTRP

Steady-state kinetic studies were conducted at variable concentrations of casein to determine the values of V_{max}, K_m, k_{cat}, *and* k_{cat}/K_m for the purified rFmTRP. Trypsin activity under assay condition in the presence of different concentrations of casein was measured by drawing the Lineweaver-Burke plot (Fig. 14a). The values of K_m *and* V_{max} for the enzyme were calculated to be 130.4 µg/mL and 0.06170 µg.min^{-1}, respectively. Based on the aforementioned values, the values of k_{cat} and k_{cat}/K_m calculated to be 131.8 min^{-1} and 1.01 min^{-1} µg^{-1}, respectively (Table 5).

Determination of thermodynamic parameters for rFmTRP

For this purpose, rFmTRP was added to potassium phosphate buffer (50 mM, pH 8.0) and incubated at different temperatures (20, 30, 40, 50°C) in the absence of casein. Enzyme fractions were collected at 15-minute intervals (0, 15, 30, 45, 60, and 75 min), and samples were cooled on ice for 30 minutes. The enzyme activity was then measured in the presence of 1 g/dL casein under specific assay conditions. The k_d values were determined based on the slopes of thermal inactivation plots. An Arrhenius plot was constructed using these k_d values (Fig. 13d).

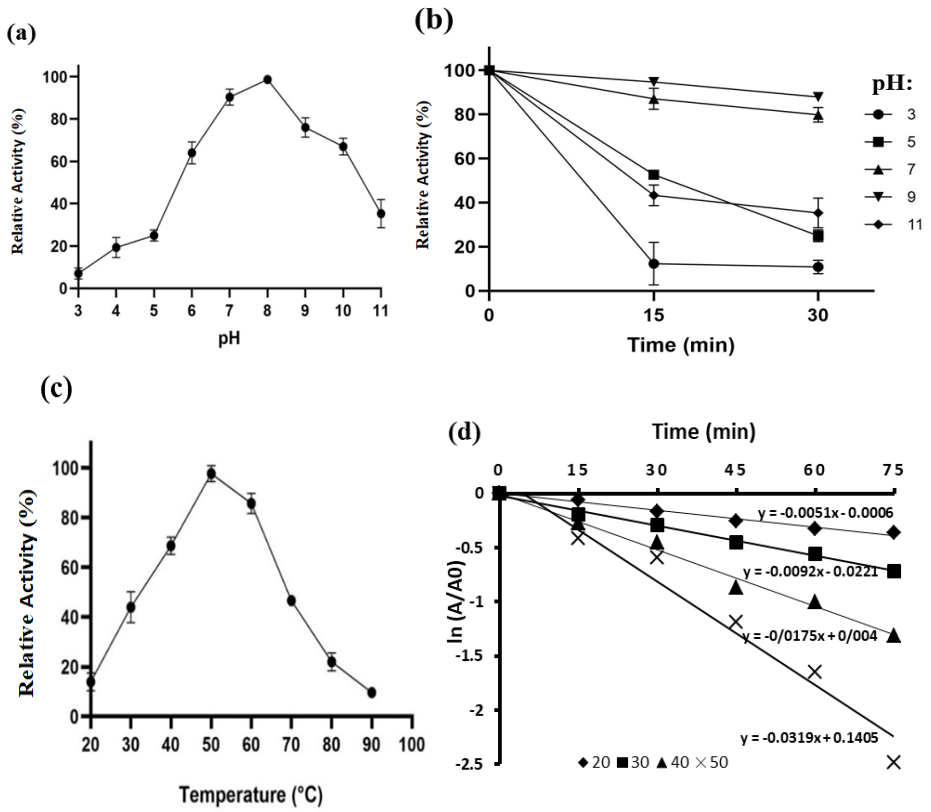

Figure 13: (a) Effect of pH on rFmTRP activity. 100% relative activity corresponds to the enzyme activity at the optimum pH. Buffers (50mM) used in assay solutions include: sodium acetate (pH 3.0–5.0), potassium phosphate (pH 6.0–8.0) and glycine (pH 9.0–10.0); (b) pH stability of rFmTRP, in pH 3,5,7,9 and 11. Control data were obtained measuring the activity of the same stock of enzyme solution incubated for the same times at room temperature; (c) Data is given as mean ±S.D. of triplicate assays. Effect of temperature on rFmTRP activity in 20-90°C range. The activity at optimal temperature was taken as 100%; (d) Determination of kd . Thermal inactivation constants can be determined from the slopes of each of the plots.

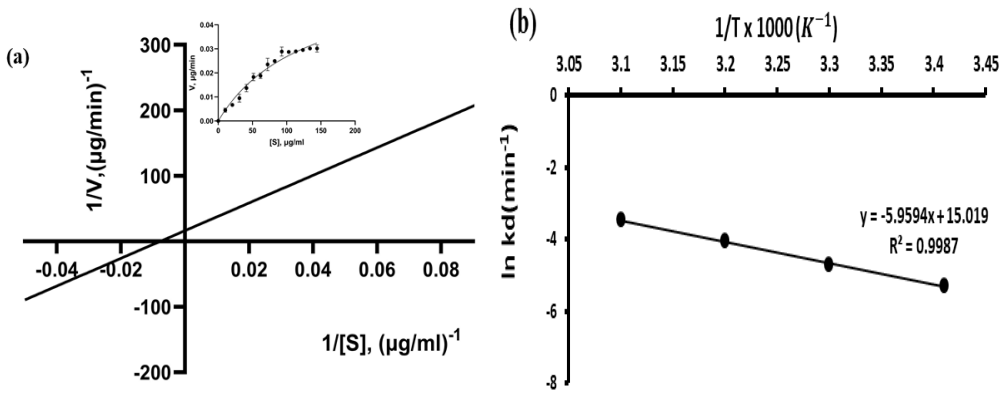

Figure 14: (a) Steady state kinetics was conducted at variable concentrations of casein to determine the kinetic parameters. The double reciprocal plot of rFmTRP activity against different casein concentrations was used to estimate K_m and V_{max} values. The inset depicts the associated Michaelis-Menten curve. Data is given as mean ±S. D. of triplicate assays. (b) Arrhenius Plot: Determination of the values of different thermodynamic parameters. To estimate $E^{\ddagger}_{a(D)}$ the natural logarithm of the values of kd versus the inverse of temperatures in Kelvin multiplied by 1000 (1/T×100) is drawn. From the slope of the equation on the plot the value of $\frac{E^{\ddagger}_{a(D)}}{R}$ is derived.

Table 5: Kinetic parameters for casein as substrate rFmTRP.

K_m (µg/mL)	V_{max} (µg.min^{-1})	k_{cat} (min^{-1})	k_{cat}/K_m (min^{-1} µg^{-1})
130.4	0.0617	131.8	1.01

The half-life (t1/2) of the enzyme at each temperature and the thermodynamic parameters were calculated based on the equations (outlined in section Thermodynamic parameters). The quantitatively calculated thermodynamic parameters for rFmTRP can be found in Table 6.

Table 6: Thermodynamic parameters for casein as substrate rFmTRP.

T (°C)	T (K)	k_d min^{-1}	ln(kd)	$t_{1/2}$ (min)	$\Delta H^{\ddagger}_D$ (kcal.mol^{-1})	$\Delta G^{\ddagger}_D$ (kcal.mol^{-1})	$\Delta S^{\ddagger}_D$ (kcal.mol^{-1}.K^{-1})	$\Delta S^{\ddagger}_D \times 1000$	$E^{\ddagger}_{a(D)}$ (kcal.mol^{-1})
20	293	0.0051	-5.2785	135.8824	11.2578	15.9820	-0.0161	-16.1235	11.840
30	303	0.0092	-4.6886	75.3261	11.2379	16.1521	-0.0162	-16.2185	
40	313	0.0175	-4.0456	39.6000	11.2181	16.2651	-0.0161	-16.1248	
50	323	0.0319	-3.4451	21.7241	11.1982	16.3792	-0.0160	-16.0404	

Following the calculation of k_d constants from the activity versus time plot (Fig. 14b), these k_d constants were utilized to construct an Arrhenius plot (ln k_d versus 1/T). The slope of the Arrhenius plot was used to estimate the activation energy of thermal deactivation ($E^{\ddagger}_{a(D)}$). The estimated value of $E^{\ddagger}_{a(D)}$ for rFmTRP was found to be 11.840kcal mol^{-1}.

As is commonly understood the value of $E^{\ddagger}_{a(D)}$ (as described by the Equation 2), is directly proportional to $\Delta H^{\ddagger}_D$. The later thermodynamic parameter is a crucial indicator of the amount of energy needed for enzyme deactivation.

The negative values of $\Delta S^{\ddagger}_D$ for rFmTRP showed negligible changes when the temperature increased from 20 to 50 °C (-0.0161 to -0.0160 kcal·mol^{-1}·K^{-1}).

As the temperature increased from 20 to 50 °C, there was an increase in $\Delta G^{\ddagger}_D$ values for rFmTRP (15.9820–16.3792).

Moreover, the t1/2 value is crucial for determining expiration and storage dates for industrial applications. Our study demonstrated a progressive decrease in t1/2 and an increase in kd with increasing temperature (Table 2), with the kd value for rFmTRP at 50 °C estimated to be 0.0319 min^{-1}, corresponding to a t1/2 of 21.72 minutes.

Effects of calcium ion on rFmTRP activity

In the current study, changes in trypsin activity at different concentrations of calcium were investigated under optimal conditions and it was found that Ca^{2+} at a concentration of 2 mM could increase the activity of *rFmTRP enzyme* by 107.3% (Table 7). It has been predicted that due to the presence of calcium-binding site (Fig. 6), *rFmTRP* was capable to bind to calcium ions.

Table 7: The effects of various concentrations of $CaCl_2$ on the activity of rFmTRP. Data is given as mean ±S. D. of triplicate assays.

concentration $CaCl_2$(mM)	Relative activity (%)
0	100±0
1	93±1
2	107.3±1.64
10	92.3± 1.5
20	80.66±1.5
40	95.66±1.5

Discussion

This study reports the purification and characterization of a novel recombinant trypsin derived from *F. merguiensis*, expressed in *E. coli Rosetta-gami*. The phylogenetic analysis revealed that *F. merguiensis* trypsin clusters closely with trypsin-like enzymes from Penaeus species, indicating a strong evolutionary relationship characterized by low genetic distances (0.03 to *P. chinensis* and 0.049 to *P. monodon*). This clustering, supported by a bootstrap value of 82%, suggests conserved functional characteristics critical for enzymatic activity (Klein *et al*., 1998; Hernández-Cortés *et al*., 1999; Kvamme *et al*., 2004; Rudenskaya *et al*., 2004). Moreover, the presence of a calcium-binding motif and key catalytic residues (His 46, Asp 97, Ser 190) further emphasizes the functional relevance of rFmTRP in proteolytic activity, aligning with findings from previous studies on arthropod trypsins (Muhlia-Almazán *et al*., 2008b; Li *et al*., 2012). The sequence alignment analysis of rFmTRP reveals significant similarity with heat-tolerant trypsins, highlighting many conserved sites. Notably, the active site includes critical residues: histidine, aspartic acid, and serine (H-D-S), specifically His46, Asp97, and Ser190, which play essential roles in catalysis (Li *et al.*, 2012). Trypsin primarily cleaves peptide bonds adjacent to basic amino acids like lysine and arginine, with its specificity determined by residues Gly216, Gly226, and Asp189, which facilitate binding and stabilize the positive charges of substrates (Stryer, 1988; Perona and Craik, 1995). The conservation of these residues across various crustaceans underscores their importance in proteolytic activity, particularly Asp212, which stabilizes the substrate-binding pocket (Fig. 6).

Secondary specificity is influenced by Try192 and Ser213, with Try192 conserved across trypsins from multiple species (Perera *et al*., 2010). Additionally, Ser190 forms a hydrogen bond with P1-Arg, affecting substrate preference (Evnin *et al*., 1990). The presence of a calcium-binding motif in decapod crustaceans, including *F. merguiensis* trypsin, raises important questions about the necessity of calcium for optimal enzyme function and stability. Our study further demonstrates that calcium significantly influences trypsin activity, with effects varying by temperature, pH, and enzyme concentration (Muhlia-Almazán *et al*., 2008b). Activation occurs at temperatures above the optimal range for trypsin (Sipos and Merkel, 1970). Previous studies have identified calcium as an activator and stabilizer for serine proteases in invertebrates, including *Cancer pagurus* and *Cherax quadricarinatus* (Figueiredo *et al*., 2001; Saborowski *et al*., 2004). In our study, we found that a concentration of 2 mM Ca^{2+} increased the activity of rFmTRP by 107.3%, highlighting its role as an activator. These findings suggest that the calcium-binding site is crucial for enzyme functionality, warranting further investigation into calcium's effects under varying conditions. Investigations into glycosylation revealed a potential N-glycosylation site at Asn55, although structural constraints make N-glycosylation unlikely. However, O-glycosylation sites at Ser18 and Thr22 were predicted, warranting further exploration. This

analysis emphasizes the intricate structural and functional characteristics of rFmTRP, contributing to our understanding of its enzymatic properties.

The values molecular size of aquatic trypsin was around 22.5–24 kDa (Haard and Simpson, 2000). When comparing the molecular weight of rFmTRP(around 23 kDa) with trypsins from other species within the Penaeidae family, our findings are consistent with reported values. For instance, trypsin from *L. vannamei* has been shown to exhibit a molecular weight of 24 kDa (Senphan *et al.*, 2015), while trypsin isolated from the digestive gland of *P. japonicus* displayed a slightly higher molecular weight of 25 kDa (Galgani *et al*., 1985). These similarities suggest that rFmTRP shares structural characteristics with other penaeid trypsins, which may indicate conserved functional roles across species. In contrast, trypsin from the hepatopancreas of freshwater prawn (*Macrobrachium rosenbergii*) had a significantly lower molecular weight of 17 kDa (Sriket *et al*., 2012). This discrepancy highlights the variability in trypsin molecular weights among different crustacean species, potentially reflecting differences in evolutionary adaptations and functional requirements in their respective environments.

The pH profile of rFmTRP reveals an optimum pH of 8 for casein hydrolysis, consistent with findings for trypsin from *L. vannamei* and *Antarctic krill*, which also exhibited optimal activity at this pH using BAPNA as a substrate (Senphan *et al*., 2015). Additionally, trypsin from *Panulirus argus* showed maximum activity at pH 7-8, while reduced activities at extremely acidic and alkaline pH values are attributed to structural changes in the enzyme (Vega-Villasante *et al*., 1995; Sriket *et al*., 2012). The pH stability of rFmTRP indicates it remains stable between pH 7.0 and 9.0, retaining about 80% relative activity, with a significant decline below pH 6 and a notable decrease at pH 3 (relative activity about 10%). Similar results have been reported for various penaeid shrimps, where trypsins are stable in neutral to alkaline pH ranges (Sriket *et al*., 2012;Wu *et al*., 2014) while instability at acidic pH is common among anionic trypsins due to lower basic amino acid residues compared to mammalian trypsin (Gates and Travis, 1969; Kim *et al*., 1994).

Optimum temperature of rFmTRP for casein hydrolysis is 50°C. However, significant activity loss occurs at temperatures above 65°C due to thermal deactivation (Khantaphant and Benjakul, 2010). Comparative studies reveal that the optimum temperature for trypsin from *P. japonicus*, *P. indicus*, and Antarctic krill is around 60°C when using BAPNA as a substrate. In contrast, rFmTRP exhibits a higher optimum temperature than many fish and shellfish, which typically range from 40 to 45°C; for instance, *P. indicus* has an optimum temperature of 45°C (Honjo *et al*., 1990), while *North Pacific krill* is reported to have an optimal range of 40-50°C (Wu *et al*., 2014). The rFmTRP maintains approximately 50% of its initial activity within a temperature range of 40 to 70°C. Thermal inactivation studies indicate that rFmTRP retains 66% and 55% of its activity after 15 and 30 minutes at 50°C, respectively. Among similar species,

trypsin from the tropical penaeid shrimp, *L. vannamei*, remains stable up to 60°C, exhibiting 95% to 99% residual activity after 15 minutes (Senphan *et al*., 2015). Conversely, trypsin from *Farfantepenaeus paulensis*, which is adapted to subtropical and temperate regions, demonstrates significant activity reduction within 15 minutes at 45°C (Buarque *et al.*, 2009). Sriket *et al*. (2012) found that trypsin from the hepatopancreas of freshwater prawns is stable up to 40°C but loses activity above 80°C. Additionally, the hepatopancreas trypsin of *P. omentaim* is stable within the 40–50 °C range for 15 minutes but rapidly loses activity at temperatures exceeding 50°C (OH *et al*., 2000).Given that the optimal temperature for rFmTRP activity is 50 °C and it maintains over 55% of its activity at this temperature for 30 minutes, it can be inferred that this enzyme is thermophile, well-suited to the warm aquatic environments inhabited by *F. merguiensis*. Steady-state kinetic studies provide valuable insights into the enzymatic efficiency and substrate affinity of rFmTRP, highlighting its potential applications in biochemical processes.

The thermal inactivation process of enzymes results in the disruption of numerous non-covalent interactions, primarily hydrophobic interactions (Sizer, 1943; Vieille and Zeikus, 1996). Based on the findings, the estimated value of $E^{\ddagger}_{a(D)}$is 11.840kcal mol^{-1}, while for the alkaline caseinolytic protease from *L. vannamei*, a similar species, the value is reported to be approximately 6.5 kcal mol^{-1}(Dadshahi *et al*., 2016). The $E^{\ddagger}_{a(D)}$ change is directly proportional to $\Delta H^{\ddagger}_{D}$. $\Delta H^{\ddagger}_{D}$ is a crucial thermodynamic parameter. Higher thermal stability in enzymes is typically associated with large positive values of both $E^{\ddagger}_{a(D)}$ and $\Delta H^{\ddagger}_{D}$ (Sizer, 1943; Vieille and Zeikus, 1996). Furthermore, the successful formation of the transition state or activated complex between the enzyme and substrate correlates with lower magnitudes of changes in the enthalpy of thermal deactivation (Joshi *et al*., 2015; Dadshahi *et al*., 2016; Ibrahim *et al*., 2021; Ortega *et al*., 2022). The negative $\Delta S^{\ddagger}_{D}$ value change indicates that the partially unfolded transition state is more structured than the native ground state, likely due to ordered cage-like structures of water molecules forming around non-polar amino acids during protein unfolding (Siddiqui, 2017; Ortega *et al*., 2022). These negative values are associated with the formation of hydrogen bonds and non-covalent interactions, including van der Waals forces (Ross and Subramanian, 1981). The increase in the value of $\Delta G^{\ddagger}_{D}$ with positive sign at higher temperatures indicates the higher thermal stability of the enzyme (Agbo *et al.*, 2017). The value of $t1_{/2}$ (enzyme half-life) is a crucial factor with economic significance as it enables the determination of expiration and storage dates for industrial or environmental uses, depending on the conditions. This is because the thermal stability increases with an increase in half-life ($t_{1/2}$) (Ahmed *et al*., 2019). Our study demonstrated a progressive decrease in the $t_{1/2}$ and an increase in k_d with increasing temperature (Table 2). This indicates a faster inactivation of the enzyme at higher temperatures. The values of k_d obtained for

rFmTRP at 50°C is estimated to be 0.0319 min^{-1}, while the corresponding $t_{1/2}$ value is 21.72 min.

Conclusions

In the present work, we identified a putative trypsin encoding cDNA from *F. merguiensis* hepatopancreas and produced rFmTRP, recombinant *F. merguiensis* trypsin, in *E. coli Rosetta-gami* for the first time. This sequence shows a high similarity to trypsins from related species in the Penaeidae family. Due to some notable characteristics such as thermal stability, optimum temperature of 50 C and tolerance to alkaline pH conditions this recombinant trypsin can be used in biotechnology and related industries. The solubility of novel recombinant tryspin needs to be improved using different strategies such as fusion protein technology and immobilization on nanomaterials (Eilerts, 2017). However, the novel trypsin from *F. merguiensis* shows the suitable activity, stability and special properties that are required for industrial applications (Bhatia *et al*., 2021). Furthermore, the novel trypsin is important from the point of view of physiology and provides more detail concerning the properties of trypsin in *F. merguiensis*.

Acknowledgments

The authors wish to thank Dr.Mahboobeh Nazari for providing bacterial hosts.

Conflicts of interest

The authors have no conflicts of interest to declare.

References

Agbo, K., Okwuenu, P., Ezugwu, A., Eze, S. and Chilaka, F., 2017. Thermostability and thermodynamic characterization of sprouted pearl millet?-amylases for its biotechnological applications. *Bangladesh Journal of Scientific and Industrial Research*, 52(**3**), 159-166. DOI:10.3329/bjsir.v52i3.34146

Ahmed, S.A., Saleh, S.A., Abdel-Hameed, S.A. and Fayad, A.M., 2019. Catalytic, kinetic and thermodynamic properties of free and immobilized caseinase on mica glass-ceramics. *Heliyon*, 5(**5**), e01674 . DOI:10.1016/j.heliyon.2019.e01674

Altschul, S.F., Madden, T.L., Schäffer, A.A., Zhang, J., Zhang, Z., Miller, W. and Lipman, D.J., 1997. Gapped BLAST and PSI-BLAST: a new generation of protein database search programs. *Nucleic Acids Research*, 25(**17**), 3389-3402. DOI:10.1093/nar/25.17.3389. DOI:10.1093/nar/25.17.3389

Bhatia, S.K., Vivek, N., Kumar, V., Chandel, N., Thakur, M., Kumar, D., Yang, Y.H., Pugazendhi, A. and Kumar, G., 2021. Molecular biology interventions for activity improvement and production of industrial enzymes. *Bioresource Technology*, 324, 124596. DOI:10.1016/j.biortech.2020.124596.

Bjellqvist, B., Hughes, G.J., Pasquali, C., Paquet, N., Ravier, F., Sanchez, J.C., Frutiger, S. and Hochstrasser, D., 1993. The focusing positions of polypeptides in immobilized pH gradients can be predicted from their amino acid sequences. *Electrophoresis*,

14(**1**), 1023-1031. DOI:10.1002/elps.11501401163

Bradford, M.M., 1976. A rapid and sensitive method for the quantitation of microgram quantities of protein utilizing the principle of protein-dye binding. *Analytical Biochemistry*, 72(**1-2**), 248-254. DOI:10.1016/0003-2697(76)90527-3

Buarque, D.S., Castro, P.F., Santos, F.M.S., Lemos, D., Júnior, L.B.C. and Bezerra, R.S., 2009. Digestive peptidases and proteinases in the midgut gland of the pink shrimp *Farfantepenaeus paulensis* (Crustacea, Decapoda, Penaeidae). *Aquaculture Research*, 40(**7**), 861-870. DOI:10.1111/j.1365-2109.2009.02183.x

Dadshahi, Z., Homaei, A., Zeinali, F., Sajedi, R.H. and Khajeh, K., 2016. Extraction and purification of a highly thermostable alkaline caseinolytic protease from wastes Penaeus vannamei suitable for food and detergent industries. *Food Chemistry*, 202, 110-115. DOI:10.1016/j.foodchem.2016.01.104

Dhani, A.K., Marsan, E.B., Kembaren, D.D., Mansur, M. and Rotinsulu, C., 2020. Reproductive Aspects of Banana Prawn (*Fenneropenaeus merguiensis*) For Recommendations of The South Sorong MPA Zone. *Journal of Fisheries and Marine Research*, 4(**1**), 150-158.

Eilerts, D., 2017. Recombinant Expression and Potential Autocatalysis of Aedes aegypti Trypsin-like Serine Proteases (AaSPII and AaSPIV). San Jose State University, Master's Theses . P. DOI:10.31979/etd.5tk2-fsj5

Eilertsen, J., Stroberg, W. and Schnell, S., 2018. A theory of reactant-stationary kinetics for a mechanism of zymogen activation. *Biophysical Chemistry*, 242, 34-44. DOI:10.1016/j.bpc.2018.08.003

Evnin, L.B., Vásquez, J.R. and Craik, C.S., 1990. Substrate specificity of trypsin investigated by using a genetic selection. *Proceedings of the National Academy of Sciences*, 87(**17**), 6659-6663. DOI:10.1073/pnas.87.17.6659

Figueiredo, M., Kricker, J. and Anderson, A., 2001. Digestive enzyme activities in the alimentary tract of redclaw crayfish, *Cherax quadricarinatus* (Decapoda: Parastacidae). *Journal of Crustacean Biology*, 21(**2**), 334-344. DOI:10.1163/20021975-99990133

Fodor, K., Harmat, V., Hetényi, C., Kardos, J., Antal, J., Perczel, A., Patthy, A., Katona, G. and Gráf, L., 2005. Extended intermolecular interactions in a serine protease–canonical inhibitor complex account for strong and highly specific inhibition. *Journal of Molecular Biology*, 350(**1**), 156-169. DOI:10.1016/j.jmb.2005.04.039

Friedman, I.S. and Fernández-Gimenez, A.V., 2023. State of knowledge about biotechnological uses of digestive enzymes of marine fishery resources: A worldwide systematic review. *Aquaculture and Fisheries*. DOI:10.1016/j.aaf.2023.01.002

Galgani, F., Benyamin, Y. and Van Wormhoudt, A., 1985. Purification, properties and immunoassay of trypsin from the shrimp *Penaeus japonicus*. *Comparative Biochemistry and*

Physiology Part B: Comparative Biochemistry, 81(**2**), 447-452. DOI:10.1016/0305-0491(85)90340-2

Gates, B. and Travis, J., 1969. Isolation and comparative properties of shrimp trypsin. *Biochemistry*, 8(**11**), 4483-4489. DOI:10.1021/bi00839a039

Ghattavi, S. and Homaei, A., 2023. Marine enzymes: Classification and application in various industries. *International Journal of Biological Macromolecules*, 230, 123136.

Gibson, R., 1979. The decapod hepatopancreas. *Oceanogr. Mar. Biol. Ann. Rev.*, 17, 285-346.

Gimenez, A.F., Garcıa-Carreno, F., Del Toro, M.N. and Fenucci, J.L., 2001. Digestive proteinases of red shrimp *Pleoticus muelleri* (Decapoda, Penaeoidea): partial characterization and relationship with molting. *Comparative Biochemistry and Physiology Part B: Biochemistry and Molecular Biology*, 130(**3**), 331-338. DOI:10.1016/S1096-4959(01)00437-7

Guerrero-Olazarán, M., Castillo-Galván, M., Gallegos-López, J.A., Fuentes-Garibay, J.A. and Viader-Salvadó, J.M., 2019. Biochemical characterization of recombinant *Penaeus vannamei* trypsinogen. *Comparative Biochemistry and Physiology Part B: Biochemistry and Molecular Biology*, 238, 110337. DOI:10.1016/j.cbpb.2019.110337

Haard, N.F. and Simpson, B.K., 2000. Seafood enzymes: utilization and influence on postharvest seafood quality. CRC Press. DOI:10.1201/9781482289916

Harp, P.M. and Li, W.H., 1987. The codon adaptation index—a measure of directional synonymous codon usage bias, and its potential applications. *Nucleic Acids Research*, 15:1281–1295

Hebditch, M., Carballo-Amador, M.A., Charonis, S., Curtis, R. and Warwicker, J., 2017. Protein–Sol: a web tool for predicting protein solubility from sequence. *Bioinformatics*, 33(**19**), 3098-3100. DOI:10.1093/bioinformatics/btx345

Hernández, J.C.S. and Murueta, J.H.C., 2009. Activity of trypsin from *Litopenaeus vannamei*. *Aquaculture*, 290(**3-4**), 190-195. DOI:10.1016/j.aquaculture.2009.02.034

Hernández-Cortés, P., Cerenius, L., García-Carreño, F. and Söderhäll, K., 1999. Trypsin from Pacifastacus leninsculus hepatopancreas: purification and cDNA cloning of the synthesized zymogen. Walter de Gruyter. DOI:10.1515/BC.1999.065

Honjo, I., Kimura, S. and Nonaka, M., 1990. Purification and characterization of trypsin-like enzyme from shrimp *Penaeus indicus*. *Nippon Suisan Gakkaishi*, 56(**10**), 1627-1634. DOI:10.2331/suisan.56.1627

Ibrahim, E., Mahmoud, A., Jones, K.D., Taylor, K.E., Hosseney, E.N., Mills, P.L. and Escudero, J.M., 2021. Kinetics and thermodynamics of thermal inactivation for recombinant *Escherichia coli* cellulases, cel12B, cel8C, and polygalacturonase, peh28; biocatalysts for biofuel precursor production. *The Journal of*

Biochemistry, 169(**1**), 109-117. DOI:10.1093/jb/mvaa097

Joshi, M., Nerurkar, M. and Adivarekar, R., 2015. Characterization, kinetic, and thermodynamic studies of marine pectinase from *Bacillus subtilis*. *Preparative Biochemistry and Biotechnology*, 45(**3**), 205-220. DOI:10.1080/10826068.2014.907181

Khantaphant, S. and Benjakul, S., 2010. Purification and characterization of trypsin from the pyloric caeca of brownstripe red snapper (*Lutjanus vitta*). *Food Chemistry*, 120(**3**), 658-664. DOI:10.1016/j.foodchem.2009.09.098

Kim, H., Meyers, S.P., Pyeun, J. and Godber, J.S., 1994. Enzymatic properties of anionic trypsins from the hepatopancreas of crayfish, *Procambarus clarkii*. *Comparative Biochemistry and Physiology Part B: Comparative Biochemistry*, 107(**2**), 197-203. DOI:10.1016/0305-0491(94)90040-X

Klein, B., Le Moullac, G., Sellos, D. and Van Wormhoudt, A., 1996. Molecular cloning and sequencing of trypsin cDNAs from *Penaeus vannamei* (Crustacea, Decapoda): use in assessing gene expression during the moult cycle. *The International Journal of Biochemistry & Cell Biology*, 28(**5**), 551-563. DOI:10.1016/1357-2725(95)00169-7.

Klein, B., Sellos, D. and Van Wormhoudt, A., 1998. Genomic organisation and polymorphism of a crustacean trypsin multi-gene family. *Gene*, 216(**1**), 123-129. DOI:10.1016/S0378-1119(98)00331-X

Klomklao, S., Benjakul, S., Visessanguan, W., Simpson, B.K. and Kishimura, H., 2005. Partitioning and recovery of proteinase from tuna spleen by aqueous two-phase systems. *Process Biochemistry*, 40(**9**), 3061-3067. DOI:10.1016/j.procbio.2005.03.009

Klomklao, S., 2008. Digestive proteinases from marine organisms and their applications. *Songklanakarin Journal of Science & Technology*, 30(**1**), 37-6.

Kumar, S., Tamura, K. and Nei, M., 2004. MEGA3: integrated software for molecular evolutionary genetics analysis and sequence alignment. *Briefings in Bioinformatics*, 5(**2**), 150-163. DOI: 10.1093/bib/5.2.150

Kvamme, B.O., Skern, R., Frost, P. and Nilsen, F., 2004. Molecular characterisation of five trypsin-like peptidase transcripts from the salmon louse (*Lepeophtheirus salmonis*) intestine. *International Journal for Parasitology*, 34(**7**), 823-832. DOI:10.1016/j.ijpara.2004.02.004

Laemmli, U.K., 1970. Cleavage of structural proteins during the assembly of the head of bacteriophage T4. *Nature*, 227(**5259**), 680-685. DOI:10.1038/227680a0

Li, Q., Cui, Z., Liu, Y., Wang, S. and Song, C., 2012. Three clip domain serine proteases (cSPs) and one clip domain serine protease homologue (cSPH) identified from haemocytes and eyestalk cDNA libraries of swimming crab *Portunus trituberculatus*. *Fish & Shellfish Immunology*, 32(**4**), 565-571. DOI:10.1016/j.fsi.2012.01.006

Li, C., Wang, F., Aweya, J.J., Yao, D., Zheng, Z., Huang, H., Li, S. and

Zhang, Y., 2018. Trypsin of *Litopenaeus vannamei* is required for the generation of hemocyanin-derived peptides. *Developmental & Comparative Immunology,* 79, 95-104. DOI:10.1016/j.dci.2017.10.015

Lu, P.J., Liu, H.C. and Tsai, I.H., 1990. The midgut trypsins of shrimp (*Penaeus monodon*). High efficiency toward native protein substrates including collagens Biol. Chem. Hoppe-Seyler, 371, 851-859. DOI:10.1515/bchm3.1990.371.2.851

Madeira, F., Park, Y.M., Lee, J., Buso, N., Gur, T., Madhusoodanan, N., Basutkar, P., Tivey, A.R.N., Potter, S.C., Finn, R.D. and Lopez, R., 2019. The EMBL-EBI search and sequence analysis tools APIs in 2019. *Nucleic Acids Research,* 47(**1**), 636-641. DOI:10.1093/nar/gkz268. DOI:10.1093/nar/gkz268

Muhlia-Almazán, A., Sánchez-Paz, A. and García-Carreño, F.L., 2008a. Invertebrate trypsins: a review. *Journal of Comparative Physiology B,* 178(**6**), 655-672.

Muhlia-Almazán, A., Sánchez-Paz, A. and García-Carreño, F.L., 2008b. Invertebrate trypsins: a review. *Journal of Comparative Physiology B,* 178, 655-672. DOI:10.1007/s00360-008-0263-y

Oh, E.S., Kim, D.S., Kim, J.H. and Kim, H.R., 2000. Enzymatic properties of a protease from the hepatopancreas of shrimp, *Penaevs omentaim*. *Journal of Food Biochemistry,* 24(**3**), 251-264. DOI:10.1111/j.1745-4514.2000.tb00699.x

Ortega, N., Sáez, L., Palacios, D. and Busto, M.D., 2022. Kinetic Modeling, Thermodynamic approach and molecular dynamics simulation of thermal inactivation of lipases from *Burkholderia cepacia* and *Rhizomucor miehei*. *International Journal of Molecular Sciences,* 23(**12**), 6828. DOI:10.3390/ijms23126828

Perera, E., Pons, T., Hernandez, D., Moyano, F.J., Martínez-Rodríguez, G. and Mancera, J.M., 2010. New members of the brachyurins family in lobster include a trypsin-like enzyme with amino acid substitutions in the substrate-binding pocket. *The FEBS Journal,* 277(**17**), 3489-3501. DOI:10.1111/j.1742-4658.2010.07751.x

Perera, E., Rodríguez-Viera, L., Perdomo-Morales, R., Montero-Alejo, V., Moyano, F.J., Martínez-Rodríguez, G. and Mancera, J.M., 2015. Trypsin isozymes in the lobster Panulirus argus (Latreille, 1804): from molecules to physiology. *Journal of Comparative Physiology B,* 185, 17-35. DOI:10.1007/s00360-014-0851-y

Perera, E., Rodriguez-Viera, L., Montero-Alejo, V. and Perdomo-Morales, R., 2020. Crustacean proteases and their application in debridement. *Tropical Life Sciences Research,* 31(**2**), 187. DOI:10.21315/tlsr2020.31.2.10

Perona, J.J. and Craik, C.S., 1995. Structural basis of substrate specificity in the serine proteases. *Protein Science,* 4(**3**), 337-360. DOI:10.1002/pro.5560040301

Rawlings, N.D., Barrett, A.J., Thomas, P.D., Huang, X., Bateman, A. and Finn, R.D., 2018. The MEROPS

database of proteolytic enzymes, their substrates and inhibitors in 2017 and a comparison with peptidases in the PANTHER database. *Nucleic Acids Research*, 46(**D1**), D624-D632.

Ross, P.D. and Subramanian, S., 1981. Thermodynamics of protein association reactions: forces contributing to stability. *Biochemistry*, 20(**11**), 3096-3102. DOI:10.1021/bi00514a017

Rudenskaya, G.N., Kislitsin, Y.A. and Rebrikov, D.V., 2004. Collagenolytic serine protease PC and trypsin PC from king crab *Paralithodes camtschaticus*: cDNA cloning and primary structure of the enzymes. *BMC structural Biology*, 4, 1-9. DOI:10.1186/1472-6807-4-2

Saborowski, R., Sahling, G., Del Toro, M.N., Walter, I. and Garcıa-Carreno, F., 2004. Stability and effects of organic solvents on endopeptidases from the gastric fluid of the marine crab Cancer pagurus. *Journal of Molecular Catalysis B: Enzymatic*, 30(**3-4**), 109-118. DOI:10.1016/j.molcatb.2004.04.002

Sainz, J.C., García-Carreño, F., Sierra-Beltrán, A. and Hernández-Cortés, P., 2004. Trypsin synthesis and storage as zymogen in the midgut gland of the shrimp *Litopenaeus vannamei*. *Journal of Crustacean Biology*, 24(**2**), 266-273. DOI:10.1651/C-2423

Saitou, N. and Nei, M., 1987. The neighbor-joining method: a new method for reconstructing phylogenetic trees. *Molecular Biology and Evolution*, 4(**4**), 406-425. DOI:10.1093/oxfordjournals.molbev.a040454. DOI: 10.1093/oxfordjournals.molbev.a040454

Senphan, T., Benjakul, S. and Kishimura, H., 2015. Purification and Characterization of Trypsin from Hepatopancreas of P acific White Shrimp. *Journal of Food Biochemistry*, 39(**4**), 388-397. DOI:10.1111/jfbc.12147

Siddiqui, K.S., 2017. Defying the activity–stability trade-off in enzymes: taking advantage of entropy to enhance activity and thermostability. *Critical Reviews in Biotechnology*, 37(**3**), 309-322. DOI:10.3109/07388551.2016.1144045

Sievers, F. and Higgins, D.G., 2018. Clustal Omega for making accurate alignments of many protein sequences. *Protein Science*, 27(**1**), 135-145. DOI:10.1002/pro.3290

Simpson, B.K., 2000. Digestive proteinases from marine animals. *Food Science and Technology-New York-Marcel*, 191-214.

Sipos, T. and Merkel, J.R., 1970. Effect of calcium ions on the activity, heat stability, and structure of trypsin. *Biochemistry*, 9(**14**), 2766-2775. DOI: 10.1021/bi00816a003

Sizer, I.W., 1943. Effects of temperature on enzyme kinetics. *Advances in Enzymology and Related Areas of |Molecular Biology*, 3, 35-62. DOI:10.1002/9780470122488.ch2

Sriket, C., Benjakul, S., Visessanguan, W., Hara, K., Yoshida, A. and Liang, X., 2012. Low molecular weight trypsin from hepatopancreas of freshwater prawn (*Macrobrachium rosenbergii*): Characteristics and biochemical properties. *Food Chemistry*, 134(**1**), 351-358. DOI:10.1016/j.foodchem.2012.02.173

Stryer, L., 1988. Protein conformation, dynamics, and function. *Biochemistry; WH Freeman and Co.: New York, NY, USA*, 143-314.

Sun, N., Lee, S. and Song, K.B., 2002. Effect of high-pressure treatment on the molecular properties of mushroom polyphenoloxidase. *LWT-Food Science and Technology*, 35(**4**), 315-318. DOI:10.1006/fstl.2001.0871

Tidwell, J.H. and Allan, G.L., 2015. Ecological and economic impacts and contributions of fish farming and capture fisheries'. DOI:10.1093/embo-reports/kve236

Vance, D.J. and Rothlisberg, P.C., 2020. The biology and ecology of the banana prawns: *Penaeus merguiensis* de Man and *P. indicus* H. Milne Edwards. *Advances in Marine Biology: Vol. 1*: Elsevier, 1-139. DOI:10.1016/bs.amb.2020.04.001

Vega-Villasante, F., Nolasco, H. and Civera, R., 1995. The digestive enzymes of the Pacific brown shrimp *Penaeus californiensis*—II. Properties of protease activity in the whole digestive tract. *Comparative Biochemistry and Physiology Part B: Biochemistry and Molecular Biology*, 112(**1**), 123-129. DOI:10.1016/0305-0491(95)00039-B

Viader-Salvadó, J.M., Fuentes-Garibay, J.A., Castillo-Galván, M., Iracheta-Cárdenas, M.M., Galán-Wong, L.J. and Guerrero-Olazarán, M., 2013. Shrimp (*Litopenaeus vannamei*) trypsinogen production in *Pichia pastoris* bioreactor cultures. *Biotechnology Progress*, 29(**1**), 11-16. DOI:10.1002/btpr.1646

Vieille, C. and Zeikus, J.G., 1996. Thermozymes: identifying molecular determinants of protein structural and functional stability. *Trends in Biotechnology*, 14(**6**), 183-190. DOI:10.1016/0167-7799(96)10026-3

Wilson, C.M., 1983. Staining of proteins on gels: Comparisons of dyes and procedures. *Methods in Enzymology*: Elsevier, 236-247. DOI:10.1016/S0076-6879(83)91020-0

Wu, Z., Wang, J., Shang, X., Yang, Z. and Jiang, G., 2014. Purification and characterization of cold adapted trypsins from Antarctic krill (*Euphausia superba*). *International Journal of Peptide Research and Therapeutics*, 20, 531-543. DOI:10.1007/s10989-014-9415-y

Yang, J. and Zhang, Y., 2015. I-TASSER server: new development for protein structure and function predictions. *Nucleic acids research*, 43(**W1**), W174-W181. DOI:10.1093/nar/gkv342

Zhou, L., Wu, J., Hu, X., Zhi, X. and Liao, X., 2009. Alterations in the activity and structure of pectin methylesterase treated by high pressure carbon dioxide. *Journal of Agricultural and Food Chemistry*, 57(**5**), 1890-1895. DOI:10.1021/jf803501q